SBIR- 08.15-1315
release date-12/17/88 ✓

Development of Moored Oceanographic Spectroradiometer
Final Report
NASA Contract Number NAS7-934

June 30, 1987

(NASA-CR-190883) DEVELOPMENT OF MOORED OCEANOGRAPHIC SPECTRORADIOMETER Final Report (Biospherical Instruments) 69 p

N93-13708

Unclas

G3/48 0121208

Charles R. Booth, Principal Investigator
B. Greg Mitchell, O. Holm-Hansen Associated Investigators
Biospherical Instruments Inc.
4901 Morena Blvd. Suite 1003
San Diego, California 92117
(619) 270-1315

Biospherical Technical Reference 87-1

Biospherical Instruments Inc.
Final Report on Moored Spectroradiometers

I. Introduction

Biospherical Instruments has successfully completed a NASA sponsored SBIR (Small Business Innovational Research Program) project to develop spectroradiometers capable of being deployed in the ocean for long periods of time. The completion of this project adds a valuable tool for the calibration of future spaceborne ocean color sensors and enables oceanographers to extend remote sensing optical techniques beyond the intermittent coverage of spaceborne sensors.

Highlights of the project include two moorings totaling 8 months generating extensive sets of optical, biological, and physical data sets in the ocean off La Jolla, California, and a 70 day operational deployment of the resulting commercial product by the ONR and NASA sponsored BIOWATT program. Based on experience gained in these moorings, Biospherical Instruments has developed a new line of spectroradiometers designed to support the oceanographic remote sensing missions of NASA, the Navy, and various oceanographers.

I.A. Background:

Measurement of oceanic optical properties, both from space and in situ, provide scientists and ecologists with an important tool for investigating a variety of problems which include estimating global algal biomass, global productivity, the role of ocean biota in global CO_2 cycles, impact of overfishing, and other anthropogenic inputs. Other areas of interest in marine optics include military applications such as antisubmarine warfare and communications. The utility of such measurements is greatly increased if instruments are available that are easily deployed from a variety of platforms or are suitable for deployment for long periods of unattended operation.

Monitoring global productivity is a key issue in resource allocation and utilization. The oceans are increasingly being looked towards as a source of food. The understanding of temporal and spatial variability of productivity in the ocean has been identified as a relevant critical issue. Spaceborne optical sensors such as the Coastal Zone Color Scanner (CZCS) have been used to determine the approximate concentration of chlorophyll in the upper waters, and with decreased accuracy, water column chlorophyll. The linkage between satellite remote sensed chlorophyll and directly measured water column productivity has been described (Smith, et.al, 1982a) and the necessity of in situ calibration to improve the predictability has been stressed.

Satellite coverage of the oceans in the visible region of the spectrum will probably never be continuous due to the limitations of cloud cover which is frequently more pronounced in areas of high productivity. In describing the period when the Costal Zone Color Scanner was operational, the MAREX report (1982) estimated that at the most only 10-20 usable CZCS images per month were produced. Gaps of several weeks to several months (at latitudes above 40 degrees) frequently occurred.

Furthermore, the high degree of spatial and temporal variability in the ocean limits satellite coverage to the macro scale and does not yet permit by itself three dimensional detailed analysis of vertical mixing (advection and upwelling). Improvements should be made in the future in this direction and supporting in situ optical instrumentation will be needed to advance future satellite sensors.

In addition to productivity estimates, monitoring of the underwater light field can provide information about the kinds and quantities of dissolved and particulate material in the water. This can in turn provide needed information on the nature and variability of the standing crop of the marine plant community, a topic of interest, for example, to marine resources management. Other areas with similar needs include monitoring for pollution control and management and long term and regional environmental water quality assessment (Bukata, et.al, 1981).

The absorption of optical energy in the ocean has been studied for many reasons including monitoring the energy input to the ecosystem and determining the constituents of the water column. Measurement of photosynthetically active radiation (PAR) is routinely done in shipboard productivity studies. Reflectance spectra have been extensively measured by airborne and spaceborne sensors. Spectral measurements are increasingly being performed to give detailed optical information about the spectral attenuation of light in the ocean and its relationship to the biological community and the remote sensing of this community.

Spectroradiometers have been used in the ocean for many years (Tyler, 1966; Smith, 1981b). Instruments in the field today are typically attached to a cable and lowered over the side of a ship. Spectroradiometric measurements in the ocean have traditionally taken an hour or longer due to the temporal variability of the underwater light field (due primarily to wave focusing effects). Other problems that have complicated underwater measurements include the fragility of the optical system, calibration stability, and power requirements. Biospherical Instruments introduced the MER 1000 Series of spectroradiometers (Booth and Dustan, 1979, Smith, et.al.,1984) specifically developed to answer these problems. Ruggedly designed, featuring no moving parts and scan times of 10-24 milliseconds, it allows tens of thousands of scans to be taken in an hour and yields high spectral resolution of the properties of the ocean. This speed advantage is also of importance in view of the recent interest in the effects of short term variation in light intensity of phytoplankton photosynthesis (Marra and Heinemann, 1982). This design served as the basis of the test platforms deployed during the 1984 and 1985-6 moorings in La Jolla.

IB. Project Overview:

The development of the moored spectroradiometers involved several steps. Initially, consideration of planned deployments of moored spectroradiometers led us to examining the types of sensors that might be incorporated into such instruments. A moored spectroradiometer deployed to measure downwelling spectral irradiance was judged to have relatively little value when used alone. To obtain a measure of the diffuse attenuation coefficient ("k"), two instruments would need to be deployed at different depths. This, while yielding a single measure of spectral k, would not provide direct measures of upwelling radiance, a critical parameter for a remote sensor. Consequently, we designed a rugged array of radiance detectors for use in the first test mooring. In consultation with other investigators in ocean optics, it was felt that upwelling spectral irradiance was another valuable parameter since both more measurements of irradiance reflectance and a more robust theory to handle these measurements existed. An instrument measuring these parameters was built and deployed during April and May of 1984. This instrument will be described in detail in a following section.

The successful 1984 deployment and the granting of a second phase of support for this project by NASA, enabled us to continue in January, 1985 on the analysis of data from the previous years mooring. This analysis leads to several conclusions:

1. Radiance reflectance ratios appear to track changes in chlorophyll as measured using a strobe fluorometer. Thus upwelling radiance combined with downwelling irradiance measured spectrally provide a good indicator of chlorophyll.

2. Newly designed upwelling radiance detectors were inherently more sensitive as compared to upwelling irradiance detectors.

3. Data from the deployment (see a later section for a full description of the site) showed high variability and it was suspected that vertical nonhomogeneity in the water column reduced the correlations between the reflectances and the pigment concentrations. This was due to the upwelling signal's origination from below the shallow mixed layer, where the platform was located. Analysis of the "penetration depth" of remote sensors by Gordon and McCluney (1975) is relevant to this point. Consequently, more samples are needed to improve the correlations. Observed changes in chlorophyll of 30% in 3 minutes during the taking of a field sample suggests methods must be developed to cope with such variability. Future deployments must also cover a greater range in chlorophyll and in sediments, in order to test the methods in the full range of oceanic chlorophyll and productivity.

4. Ratios of upwelling radiance at 671nm to downwelling irradiance at 488nm also appeared to track the fluorometer based chlorophyll measurement and this needs further exploration.

5. There was a significant time varying (periods less than 1 minute) component to the data and this appeared to be related to gravity waves.

6. Bio-fouling was a considerable problem, but was resolved.

7. The sensor technology was stable over a one month period.

8. Optical moorings showed promise for becoming a powerful tool for monitoring biological variability, but a considerable amount of data was needed to develop relationships between the optical measurements and the biological components.

Following these conclusions, a second, longer mooring was planned. In this mooring we decided to deploy two instruments. One moored at a constant depth, and one periodically deployed from a skiff in a vertical profiling mode. This would provide a direct measure of the vertical optical and physical variability of the water column, and allow discrete biological samples to be obtained during the cast. In addition, we decided to add a variety of additional optical and physical sensors to this "optical test-bed" to better relate the optical measurements to commonly measured physical oceanographic properties.

To accommodate the increased number of moored sensors, we decided to build a completely new spectroradiometer (known as the MER-1064, serial number 8303) and to use the instrument from the first mooring (S/N 8302) as the starting point for the vertical profiler. This also involved adding a channel expansion unit to the unit 8302 to allow full wavelength matching with the moored unit. New engineering development preparing for this second mooring including designing hardware and software channel expansion for the MER-1032 to 64 channels, design of a thermistor chain and support electronics, interfacing of a EMCM current meter, design of small sensor packages to support a second set of two sensors below the main package, and design of integral scalar irradiance sensors for the MER.

The optical system of the testbed, and of the newly developed MER-2000 series instruments utilize a completely "solid state" electro-optical design with no moving parts to get out of alignment or calibration during the inevitable rough handling at sea. Other designs that we considered utilize a grating or prism which separates the spectrum into the various spectral components. This dispersive element is either moved mechanically, bringing the spectral components into view of either a photomultiplier or a silicon photodiode, or the spectrum is dispersed across an array of photodetectors. An example of this type of design is the "Scripps Spectroradiometer" described by Tyler and Smith (1966). Considering the first approach, in addition to the relative lack of ruggedness due to moving parts, the slow (several seconds to traverse the spectrum) scanning time will cause any surface waves to distort the recorded spectrum due to their modulation of the underwater light field. The only way to avoid this distortion is to record many scans **at each wavelength** and compute the average while holding the instrument at the same depth. This is a real disadvantage at sea.

The second approach considered, uses a fixed element to disperse the spectrum across a detector, such as a linear photodiode array or a video camera tube. The spectrum may then be electronically scanned with much higher speed than possible by mechanical means. While this is an extremely effective approach in certain applications, difficulty arises since light intensity differs by more than a hundred times across the spectrum below 10 meters depth in the ocean and much more as depth increases. The wavelength of interest may be contaminated by spectral "leakage" or "spill over" of unwanted light from much brighter parts of the spectrum. Another serious limitation is the lack of sufficient dynamic range necessary in environmental monitoring as these systems rarely have more than a 10^4 range yielding a working range of less than 1000.

The approach we chose uses an array of discrete narrow band photodiodes, each with its own precision amplifier whose gain is optimized for its wavelength and with consideration of the spectral intensity of the underwater light field. All channels are electronically scanned, autoranged and digitized. This design achieves maximum dynamic range (>10^6) and a high degree of spectral blocking that only a specially designed combination of absorbing and interference filters can provide. In addition, this system has a proven history of maintaining its calibration during intensive field use since there are no moving parts. The result is a rapid scanning, rugged and highly accurate environmental monitoring system with a typical recalibration stability, after one year of field use, within 2% (see tables in the following sections). A plot of the spectral response of the channels from a typical MER series spectroradiometer can be seen in figure 1.

Using this approach, a sampling of discrete wavelengths is obtained rather than a continuous spectral scan. This means that the users must define their needs in advance, selecting the most appropriate wavelengths for their research. For example, several pigments commonly found in marine organisms (e.g. chlorophyll, carotenoids, etc.) have well defined absorption minima and maxima. Some users select spectral bands used in satellite and aircraft remote sensing studies, laser lines, or areas where specific pollutants have strong light absorption. This approach does not permit utilization of such techniques as derivative spectroscopy which require very high resolution data.

The testbed was built around a 6802 type microprocessor controlling a 12 bit analog to digital converter with three programmable gains (1, 16, 256), giving the system a dynamic range of 1,000,000 to one. The instrument scan time for 16 analog channels is as fast as 10 milliseconds and the individual sensors have nominal time constants of 100 milliseconds, permitting a "snapshot" measurement of the spectral irradiance. The instruments also have averaging capabilities permitting up to 2048 complete scans to be averaged before the data is transmitted to the surface. Most of the data collected during the November 85-June 86 mooring was the average of 2048 scans collected over 130 seconds repeating every 150 seconds. Occasional "fast" data collection runs were obtained without scan averaging and a repetition rate of 0.4 seconds.

The newly designed mooring was deployed in November, 1985 and was removed June 23, 1986. Sampling with the vertical profiling system started in October and continued until May, 1986. During this period, the following data were collected:

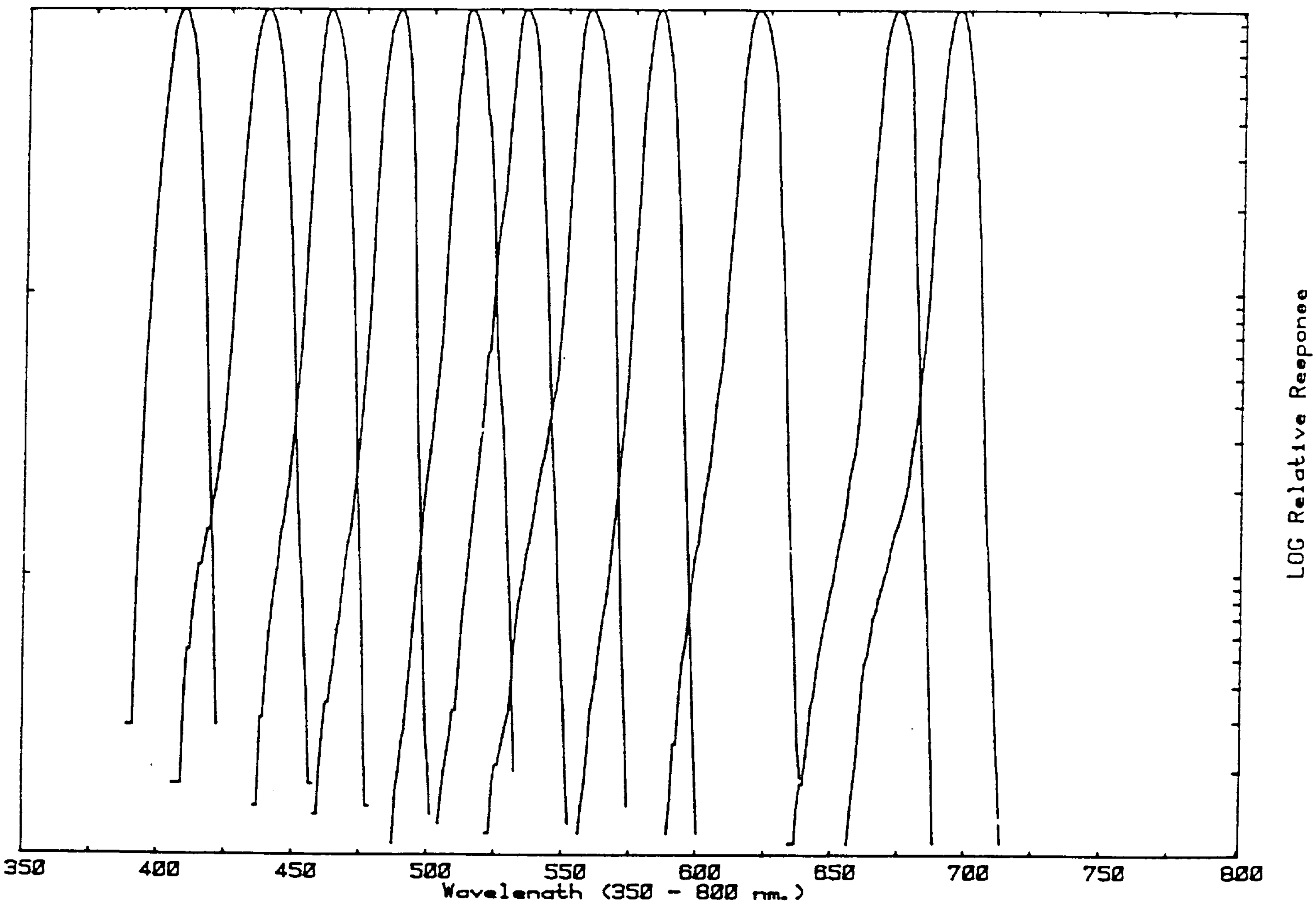

Figure 1: Multiwavelength detector spectral characteristics (log plot)

Days of data collected:	216 days
Mooring separate data sets:	200 sets
(each set is composed of a "bin" and a "das" file)	
Total size of mooring data set:	32,347,520 bytes binary packed
Vertical Profiles:	88 profiles
Vertical Profile file size:	2,043,776 bytes binary packed
Biology/Chemical Spreadsheets:	43 vertical profiles
First/last Moored Data File:	11/13/85, 06/23/87
First/last Vertical Data File:	10/15/85, 05/23/87

Analysis of these data is proceeding and is also the subject of an ongoing contract to the Scripps Institution of Oceanography. This report will present an overview of these data and focus on selected data. The success of both moorings let us develop the design criteria for the new moorable spectroradiometers (called the MER-2000 series). Some of these criteria are listed below:

1. Battery power: capacity of a minimum of three to six month deployments. It was thought that moorings longer than six months would be highly questionable due to biofouling since the moorings would almost always be in the euphotic zone.

2. Large data storage capacity: a minimum of 10 megabytes of storage.

3. A high resolution, high dynamic range, fast, low power data acquisition system (minimum of 20 bits or 1-1,000,000 dynamic range) would be required. Since none were commercially available, it would have to be developed.

4. Mechanical design would have to be rugged to survive the deployment and retrieval operations, along with resisting possibly high vibrations due to mechanical "strumming" of the mooring lines in a taut mooring.

5. Considerable flexibility in the electronics would be needed to allow a variety of sensors to be connected. Our experience in manufacturing optical systems for oceanographers has taught us that every investigator may be looking at a problem from a different viewpoint, and may require different associated sensors. Examples of these sensors would include fluorometers, transmissometers, temperature, pressure, and conductivity sensors. This would require as many as 48-64 channels.

With these goals in mind we designed the MER-2020 moorable spectroradiometer. Appendix I describes the specifications for this instrument. The first operational deployment of this instrument was in the BIOWATT program. Two MER-2020s moored at 30 and 50 meters performed flawlessly between February and May of 1987. This successful deployment concluded this NASA SBIR contract.

II. Description of the Testbed Moorings, 1984-1986

The following sections will describe the site and method of the test moorings, the instrument configurations used, the data sets collected, and representative data.

II A. Description of the La Jolla Test Site:

During both the 1984 and 1985-86 moorings the test platform was deployed by attachment to the Scripps Canyon Sea Structure. The Scripps Canyon Sea Structure, installed by R.W.Austin and the Visibility Laboratory in conjunction with K.N.Nealson of the Scripps Marine Biology Department (Warner, et.al, 1983, Nealson, et.al., 1984), is permanently installed in a tripod configuration straddling the Scripps Submarine Canyon 1000 meters seaward of the Scripps Pier (see Figures 2a & b). The main buoy for the Sea Structure is above the 600 foot isobath and anchored at a mean tide depth of 16 meters below the surface. The length of each anchor leg is approximately 137 meters. The spectroradiometer package was deployed between two of the inshore anchor legs approximately 25 meters south south-east of the main buoy. A three point tethering scheme was accomplished by attaching two lines to the anchor legs at points 45 meters from the main float. A third tethering line was run from a point 2 meters from the main float on the pier leg. This placed the spectroradiometer package approximately 120 meters over the bottom. In this method of deployment, the package had an unobstructed view for the up and down welling optical measurements. There was an insignificant obstruction of the upwelling irradiance field due to the anchor lines. Effects of the platform shading the upwelling light field are discussed later.

The deployment depth of the moorings was determined by considering the research objectives, the available mooring site, and the survivability of the instrument. To accurately measure the upwelling radiance signal that a satellite will sense, the instrument would be located at the surface. Problems encountered by a surface deployment would include maintaining the correct vertical orientation in the presence of wind and waves, avoiding collision and theft, and being able to determine the exact environment of the downwelling irradiance collector (wet or dry, clean, etc.). To avoid the above mentioned problems, the test platforms were deployed at nominally 8 meters below the surface. Actual depths ranged from 5 meters to 9 meters, accounted for by the tidal range of approximately 2.5 meters and by the change in flotation during the project.

The following sections list components of the mooring testbed for the two Scripps Canyon moorings. Table I summarizes the specifications of the testbed electronics and specifications common for both moorings. Tables II and III summarize the measured parameters for both moorings. Table IV summarizes the physical and optical properties measured by the vertical profiler during the second mooring and Table V lists the biological and chemical parameters measured with discrete bottle samples during the second mooring.

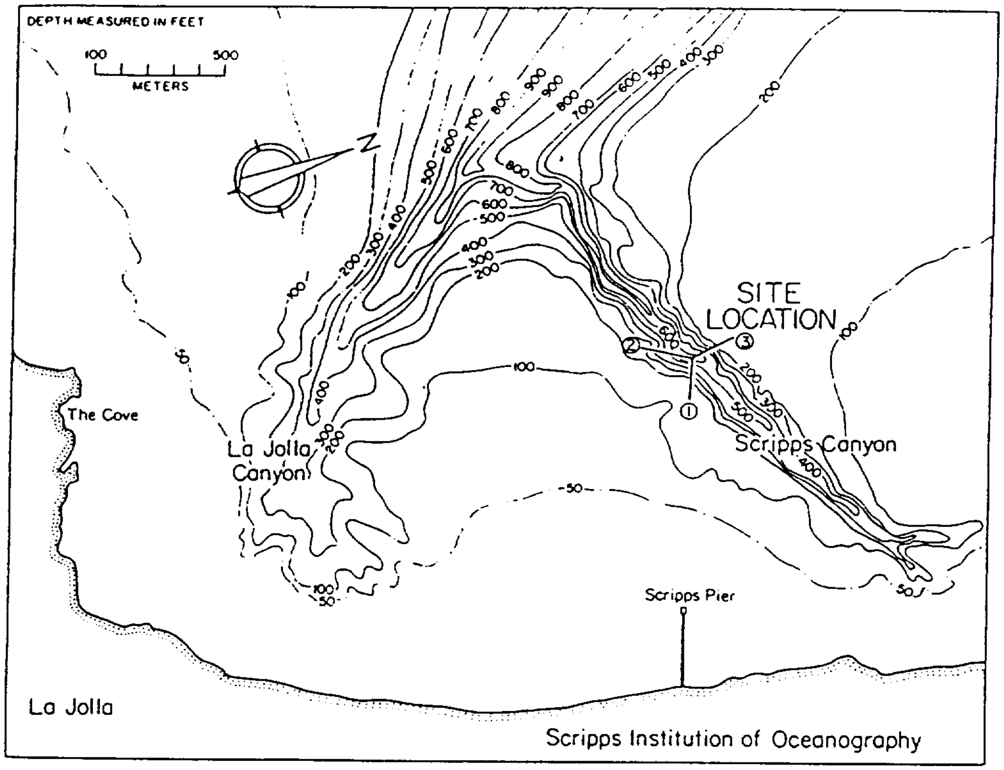

Figure 2a: Site of the Scripps Canyon moorings (from Warner, *et. al.*1983)

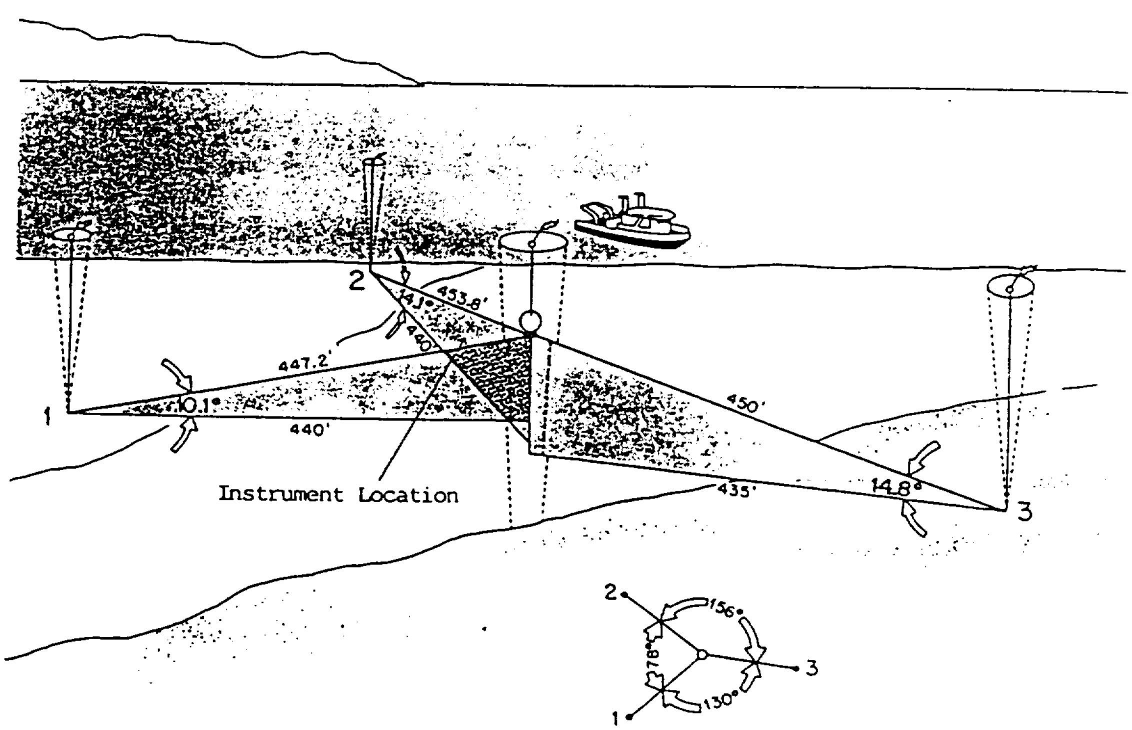

Figure 2b: Details of the Scripps Canyon Sea Structure (from Warner, *et.al.* 1983).

TABLE I: Specifications of the Spectroradiometer Development Testbed

Spectroradiometer Channels:
Wavelengths (nm.): See Tables for Each Deployment
Detectors: Silicon photodiodes, 4.6 * 4.6 mm active area
Filters: 3 cavity hermetically sealed interference filters with additional 3-6mm absorbing glass blocking filters
Field of view: Irradiance channels: 180° (cosine)
Radiance channels: 10.2° half angle in water
Bandwidth: 50% points ±5nm 1% points ±10nm
Response time: 0.1 second nominal
Wavelength Accuracy: ±3nm.
Radiometric Accuracy: 5%
Temperature Stability: (Dark reading) ±0.0001% FS/°
(Responsivity) ±0.05% of reading/°
Stray light: 0.01% 40 nm from peak
Irradiance Collector: 6.3 cm diameter acrylic (Smith, 1969)
Sensitivity: Each channel gain optimized to saturate at twice maximum expected natural light levels
Radiance Collector: Radiance field of view defined in the housing with baffles. Clear plexiglas window in housing to seawater

Data Acquisition System:
32 analog channels, 2 frequency channels. This was expanded to 64 analog channels during the 85-86 mooring.

Analog Channels:
Resolution: 12 bits, gain of 1,16,256 automatically selected
Least Significant Bit, gain=256, -4.76 microvolts
Full Scale: -5 volts (single ended)

Frequency Channels:
Input range:1000 to 50000 Hertz
Periods Averaged: 255,511,1023,2047 (software selectable)
Frequency resolution (at 10 kHz,2047 periods averaged, .21 sec interval): .004 hertz
Master Clock: 2.4576MHz, ±0.015% (0-70°)

Depth Sensor: 300 psia full scale bonded strain gauge
Pressure transducer stability: ±0.03% FS/°
Pressure accuracy: better that 0.5 %
Operational cable length: up to 8000 meters
Data acquisition,process and transmit time: .184 sec (fastest)

Temperature Sensor:
Resolution (2047 periods averaged) = 100 microdegrees
Accuracy: ±0.01248°

Conductivity Sensor:
Accuracy: 0.001 S/m Resolution: 0.00001 S/m

Transmissometer:
Wavelength: 660nm Path Length: 25 cm.
Acceptance angle: <18 milliradians Accuracy: ±0.5%
Beam Diameter: 15mm

System Power Requirements: Power was supplied from a shore mounted AC powered system during the testbed deployments. Data was recorded with a 4 Mhz Z-80 personal computer with a 5 MByte "Winchester" Disk.

TABLE II: April-May 1984 Mooring Sampled Parameters

At the underwater platform:

Downwelling Irradiance: 410, 441, 488, 520, 550, 589, 633, 656, 671, 694nm

Upwelling Irradiance: 410,441,488,520,550,589,633,671

Upwelling Radiance: 410,441,488,520,550,589,633,671

Depth
Two axis angle
Temperature*
Conductivity*
Beam Transmission*
Fluorometer***

At the end of Scripps Pier:

Downwelling Irradiance:410, 441, 488, 520, 550, 589, 633, 656, 671, 694*

Eppley Precision Spectral Pyranometer*
Eppley UV Radiometer*
Scalar Photosynthetically Active Radiation Sensor
Cosine Photosynthetically Active Radiation Sensor
Wind Speed and Direction **

Gravity waves data (significant height, period, and spectra on six hour averaged data) we obtained from M. Sessions at the Near Shore Processes Group.

* loaned by R.C.Smith, UCSB
** loaned by the Shore Processes Group and Scripps
*** loaned by the Food Chain Research Group at Scripps

TABLE III:November 1985-June 1986 Sampled Parameters

Downwelling Irradiance: 410, 441, 488, 520, 550, 560, 589, 633, 656, 671, 683, 694, 710nm
Upwelling Irradiance: 410, 441, 488, 520, 550, 589, 671, 694nm.
Upwelling Radiance: 410, 441, 488, 520, 550, 633, 656, 683nm.
Upwelling and Downwelling Scalar Irradiance: 441, 488, 550nm

Additional optical parameters included:
- PAR (Photosynthetically Active scalar Radiation)
- Solar Stimulated Fluorescence at 683nm (non-shaded)
- Beam attenuation coefficient
- Downwelling Irradiance at 441 and 550nm approximately 20 meters below the main instrument assembly.

Physical Parameters measured included:
- Pressure (for depth of the instruments)
- High resolution Temperature
- Conductivity
- Water current in two directional components
- Angle of the platform in two directional components
- Temperature at 3 points above and 12 points below the platform. Each point separated by 1.5 meters.

In addition to these parameters, PAR was measured with both cosine and scalar response sensors on the end of the Scripps pier located approximately one kilometer from the mooring. Solar zenith and azimuth angles were continuously calculated and appended to the data set.

TABLE IV: Sensors on the vertical profiling package October 1985-May 1986

Downwelling Irradiance: 410, 441, 488, 520, 550, 560, 589, 633, 656, 671, 683, 694, 710nm
Upwelling Irradiance: 410, 441, 488, 520, 550, 589, 671, 694nm.
Upwelling Radiance: 410, 441, 488, 520, 550, 633, 656, 683nm.

Additionally, the following optical parameters were measured:
- PAR (Photosynthetically Active scalar Radiation), both at the underwater profiler, and in air at the skiff
- Beam attenuation coefficient

Physical Parameters measured included:
- Pressure (for depth of the instruments)
- High resolution Temperature
- Conductivity
- Angle of the platform in two directional components

II B. Chronology of the April-May 1984 Mooring:

The instrument was built, tested and ready for deployment by April 10, 1984. Weather conditions allowed three Scripps SCUBA divers led by Ron McConnaughey and Charlie Arneson to deploy the instrument on April 16, with sampling beginning at 18:00 hours. On 19 April part of the flotation collapsed and the platform angle increased to approximately 25 degrees from level. By 30 April the platform angle had deteriorated to 60 degrees from level. Underwater optical data acquired during this period of severe tilt is mostly useless, although the fluorometer, transmissometer, and CTD sensors along with the pier sensors are valid. Heavy seas prevented divers from adding flotation until 1 May, and from then on the platform remained at a satisfactory orientation until it was removed on 10 May.

A sampling program utilizing a small skiff with a winch for deploying Niskin bottles was provided by R.W.Eppley of the Food Chain Research Group. Samples were taken for chlorophyll and phaeopigments, and C14 productivity samples were also run. Sampling was done on 6 occasions between 18 April and 7 May. Samples were also taken for species, pigment concentration and primary analysis. There were no electronically recorded measurements from these vertical profiles.

II C. Chronology of the November-June 1986 Mooring:

This mooring design included having two spectroradiometer based systems, one moored, and one skiff based and used in a vertical profiling mode. The moored instrument was designed to have a set of deep sensors, a thermistor string and a current meter to help define changes in the water mass below the platform. This called for further expansion of the MER-1000 series of instruments to allow a total of 64 analog channels as listed in the summary of mooring channels.

The vertical profiling system was designed to be battery operated, and deployed from a 18 foot "Boston Whaler" skiff. It matched most (except the scalar) of the optical channels found in the mooring and provided a method of calibrating any change in the mooring sensors. Specifically, this system included sensors to acquire a subset of the data being acquired by the moored system. Acquired data included salinity, temperature, beam attenuation, PAR, up and downwelling spectral irradiance, and upwelling spectral radiance. Profiles down to 60 meters depth were conducted.

II C. 1. Mooring Installation and Maintenance:

The following discussion should be prefaced by noting that the mooring underwater installation and frequent maintenance was led by Ron McConnaughey of Scripps. He is responsible for the success of this aspect of the project.

The first attempt at installation occurred on November 7, 1985. The submarine cable was found to be severed at the pier due to heavy storm action. This necessitated removing the instrument package from the water and sending a diving team to inspect the underwater portion of the cable. Fortunately, the break was located and we were able to bring the cable to the surface where a professional cable splicer could be hired to make the repair. Finally, on 13 November the mooring was installed and data acquisition started. The first few days of data show higher than normal noise and some zero offset (from that of the rest of the deployment) due to a ground loop in the underwater cable which was then corrected. All systems were working except the fluorometer.

Flotation was added on 26 November to help platform stability. At this time high concentrations of isopods (possibly *Caprella laevinscula*) were noted on the mooring including the portions coated with Aquatek anti-fouling wax. This colony thrived during both moorings and was as thick as 2 cm at the end of June 1986.

On December 11, 1985 divers serviced the mooring and replaced a broken mooring line. On January 27, 1986 divers leveled the platform and an extensive set of photographs taken by Charles Arneson document the extent of fouling.

On 18 February 1986 divers repaired storm damage to the mooring lines and removed a large section of kelp which had fouled the mooring.

The flotation chambers in the mooring continued to show gradual leakage and periodic dives were made to level the platform. During these dives, any fouling by kelp or other substances were cleared. These dives occurred on the following dates: 3/1/86, 3/20/86, 4/21/86, 5/1/86, 5/14/86.

The mooring phase of the project allowed us to obtain day long records of the natural variation in the optical properties under a variety of sea state, sky conditions, and chlorophyll concentrations. The time series has been marred by periods where the average underwater platform angle was greater than 10 degrees from level. This was caused by a variety of conditions including breaking of one of three mooring lines, failure of attachment points, extensive fouling by seaweed during and after heavy storms, and loss of flotation. These incidents caused the mooring to provide less than ideal data until conditions permitted the diving team to return to the site to repair the fault.

May 14, 1986 saw the successful completion of the planned six month Moored Spectroradiometer Deployment at the Scripps Canyon Sea Structure. The mooring continued to record data until June 23, 1986, when it was removed. This last period did not have attendant skiff based sampling and fouling on the platform was heavy, so we do not consider this latter period in most of the data analysis. This marks by far the longest continuous deployment of optical instrumentation in natural waters.

II C. 2. Data Catalog: November 85-June 86 Mooring

Appendix One contains the data catalog for the November 85 to June 86 mooring. This table includes the date of the first scan, start and stop times, file name, number of scans in the file, average platform angle during the file, and the time between samples. This table lists some 200 data files.

Appendix Two contains the list of October 85-May 86 Vertical Profiles. This table lists the date of the profile with start and stop times, and the number of scans recorded. The index also references the mooring file name and record number that correspond to the vertical profile. The sky condition as observed during the profile is also noted.

II D. Calibration Stability

Electronically, the moored spectroradiometer and its integral sensors performed flawlessly throughout the mooring. Several external sensors obtained from other sources failed. This includes the strobe based fluorometer (failure of the strobe), the transmissometer (biofouling), and after six months of successful operation, the thermistor string (mechanical abrasion). Zero drift in the internal optical spectroradiometer channels has mostly shown standard deviations of 1 part per million (ppm) when a time series of one reading taken at midnight was selected for the six month time series. This is equal to the resolution of the data acquisition system. No significant correlation in any of the optical channels with temperature was found. This is notable since it justifies the extension of the dynamic range in the new spectroradiometers to be able to resolve 0.25ppm. Noise levels on external sensors were considerably higher, and were slightly correlated with time (probably due to some corrosion occurring and the overall ground potential changing). For future moorings, we strongly recommend against using external sensors where high dynamic range will be required. There are implications in this for the development of "natural fluorometers", and these will be strongly considered in that related project.

TABLE IV
CALIBRATION FACTORS BEFORE and AFTER APRIL-MAY 84 DEPLOYMENT

WL	Ed	Eu	LU
410	+2.6	+0.4	-2.5
441	+1.2	+0.4	-2.8
488	-0.1	+0.2	-1.1
520	+2.1	-2.6	-2.2
550	-2.4	-1.0	-2.6
589	+1.2	+1.4	-4.0
633	-1.3	-0.1	-4.7
656	-1.6	N/A	N/A
671	-2.6	+0.3	-2.3
694	+0.6	N/A	N/A

Calibration dates: 4/11/84, 5/15/84
Data expressed as % change

TABLE V
CALIBRATION FACTORS BEFORE and AFTER NOVEMBER 85 - JUNE 86 DEPLOYMENT

WL	Ed	Eu	Lu	Eod	Eou
410	0.8	0.5	4.1		
441	1.9	1.8	2.2	5.0	14.9
488	-0.7	2.8	1.1	20.3	3.2
520	0.6	3.1	-1.8		
550	-1.6	1.6	3.7	8.5	12.9
560	-1.9				
589	0.0	2.0			
633	-1.8		2.2		
656	1.0		6.0		
671	0.4	-0.7			
683	-0.3		4.1		
694	-4.5	-2.1			
710	-0.5				

PAR at Platform	34.0
PAR at Pier (scalar)	14.9
PAR at Pier (cosine)	-0.5
441 deep Ed	6.2
550 deep Ed	0.6
L(683)	8.0

Calibration dates: 3 Nov 85, 28 Aug 86
Data expressed as % change

II E. Biological and Chemical Sampling October 1985-May 1986

To build a data base that would help in the evaluation of the various optical sensors being tested, an extensive set of biological and chemical measurements were taken from a small skiff launched from Scripps Pier. This sampling was with 5 liter Niskin bottles deployed by winch with the MER-1048 described earlier. This aspect of the project was carried out under a subcontract to O. Holm-Hansen at Scripps and was directed by Greg Mitchell. The following is a complete list of those parameters. (Not all listed were measured on every cast.)

TABLE V: Biological and Chemical Parameters Sampled During the Second Mooring:

Observed Sea State
Observed Sky State
Start and Stop time of profile
Secchi depth

The following parameters were obtained from 6 depths each time. Not all parameters were measured on each vertical profile:
Chlorophyll *a*(mean and range)
Phaeopigments (mean and range)
HPLC pigment determinations:
Chlorophylls *a, b, c*; fucoxanthin; 19-hexanoyl-oxy-fucoxanthin; peridinin; diadinoxanthin; diatoxanthin; lutein; alpha-carotene; beta-carotene; phaeophorbide
Phycoerythrin concentration
Carbon Fixation (in situ incubation), including start and stop time of incubation
Photosynthesis-Irradiance analysis
Particle size distribution, "Coulter Counts", 16 bins
Particulate Nitrogen, Carbon concentration
Cyanobacteria counts
Seston organic, dry and ash free weights
Inorganic nutrients:
SiO_4
PO_4
NO_3
NO_3
NH_4
Absorption coefficient spectra
Fluorescence excitation and emission spectra

During the 6-months deployment of the mooring system, detailed biological analyses were conducted on 21 dates. The time series of integrated water column primary production during this period is plotted in Figure 3a. The plot reveals that during the period of the mooring, primary production varied by a factor of 5. The data set offers an ideal opportunity to test optical algorithms and models for predicting primary production from optical moorings or remote platforms.

An example of how pigment algorithms can be tested can be seen in figure 3b. This plot covers the range of chlorophyll plus phaeopigments encountered during the mooring. We have plotted chlorophyll and phaeopigment against the frequently used remote sensing ratio of reflectance at 441 and 550nm. This data set covers all depths and light levels. No filtering has been done to exclude data near the surface where there might be shadow effects from the boat, or to exclude deep data where we suspect the upwelling signals at 550nm are enhanced by fluorescence from phycoerythin. The R^2 for these data is 53%. We suspect that this can be substantially improved.

Since variability in the particulate absorption coefficient dominates variability in the spectra of K and reflectance for oceanic waters, we routinely measured particulate spectral absorption coefficients. Additionally, a continuing effort is being made to process HPLC determined pigment concentrations. This, in combination with absorption spectra and *in situ* spectral reflectance may produce improved algorithms to determine accessory and degradation pigments in addition to chlorophyll *a*.

II F. Biofouling and Corrosion

Corrosion prevention on the moorings consisted of specifying the aluminum alloy T-6061 and applying hard-coat anodize. All metal parts were kept isolated from any dissimilar metals. To do this, nylon or "Delrin" plastic bushings were placed around all fasteners. At the beginning of the November 1985 mooring an electrical ground loop between the instrument on the Sea Structure and the power supply on campus at Scripps existed and caused heavy corrosion on certain parts that were connected to "ground" in a period of 3 days. When this situation was corrected, no further corrosion occurred. One window flange exhibited significant corrosion but we have reason to believe it was not constructed from the same alloy.

In the Biowatt mooring one housing was significantly corroded but upon disassembly we noted that the insulating layer of neoprene had pinched causing some suspected contact between the 316 stainless steel frame and the MER-2020 housing. The zinc protection anodes had disappeared from this frame. The other housing was not affected and its zinc remained in place throughout the mooring.

Bio-fouling in the Scripps Canyon Mooring was suppressed with great success on the irradiance and radiance windows by using an organo-tin compound in a clear binder (called OMP-3). This material was obtained from R.W.Austin of the Visibility Laboratory who obtained it from researchers at the Navy's David Taylor Ship Center. This compound remained clear (according to diver's observations) throughout the 7 month mooring. On recovery, the windows were still clean, but most of the compound had disappeared. The platform and instrument housing was coated with a thick coating of Aquatek anti-fouling wax. Signs of this wax remained at the end of the mooring, but this may have been good substrate

substrate for the certain organisms (*Caprella laevinscula*) rather than a deterrent. By the end of the 7 month mooring the only portions of the instrument platform that were visible were the optical windows.

The teflon scalar irradiance collectors exhibited some fouling, probably caused by the frequent impact of kelp on the instrument platform. The kelp possibly rubbed the antifouling material off. The OMP compound did adhere if not abraded. The fouling materials sometimes found on these detectors could easily be brushed off and little adhered. This fouling may account for the relatively poor calibration stabilitiy of these sensors.

The Biowatt mooring used a later version of this same clear antifouling material, but problems were encountered in applying the material evenly and without clouding. Fortunately, the relatively low productivity of the Biowatt site saw little fouling even on unprotected surfaces during the first 70 day mooring.

The clear OMP compound is effective in preventing fouling, it does not affect the calibration of radiance or irradiance collectors if it is applied evenly and remains clear during the drying process. The compound may affect the calibration of transmissometers, but this is a special case because of the critical collimated beam of that instrument. The drawbacks of this compound are: 1) it is highly toxic and care must be used in application, 2) it is not commercially available, and 3) it is hard to apply. Three months moorings in oligotrophic waters should present no problems if commercial antifouling paints are applied immediately around the optical collectors, or if OMP compounds can be used. In eutrophic waters, OMP is essential for periods longer than a few weeks and it is also necessary to use good antifouling paints on the housings.

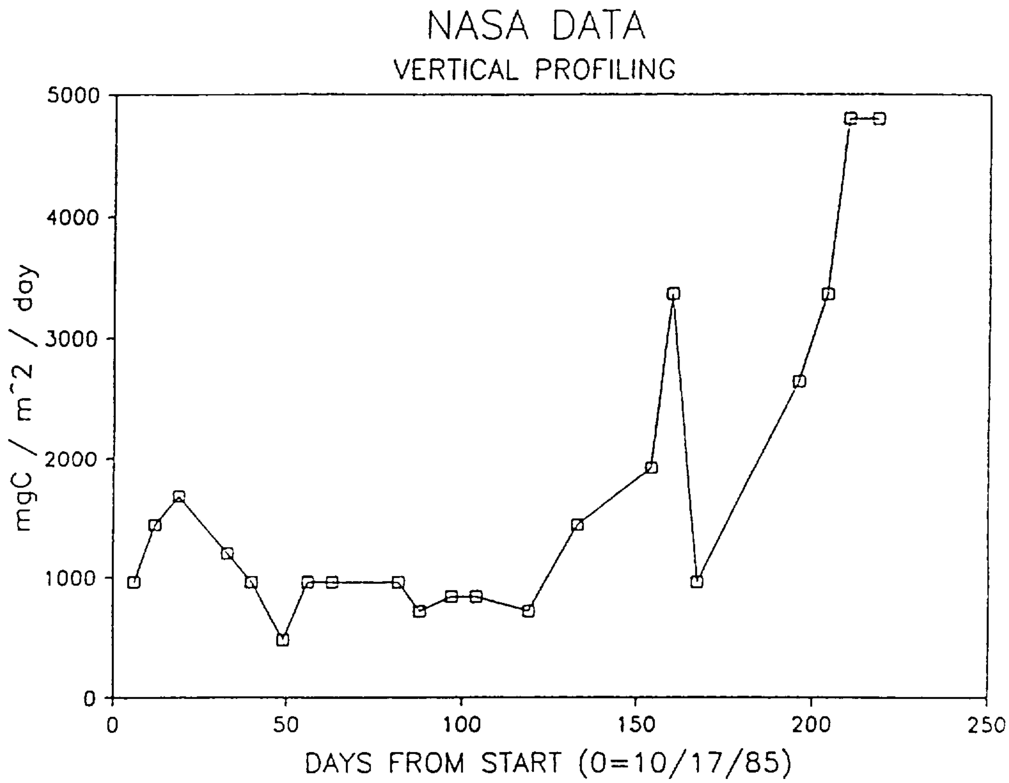

Figure 3a: Integrated water column productivity as measured throughout the mooring. A more than 5 fold variation is noted.

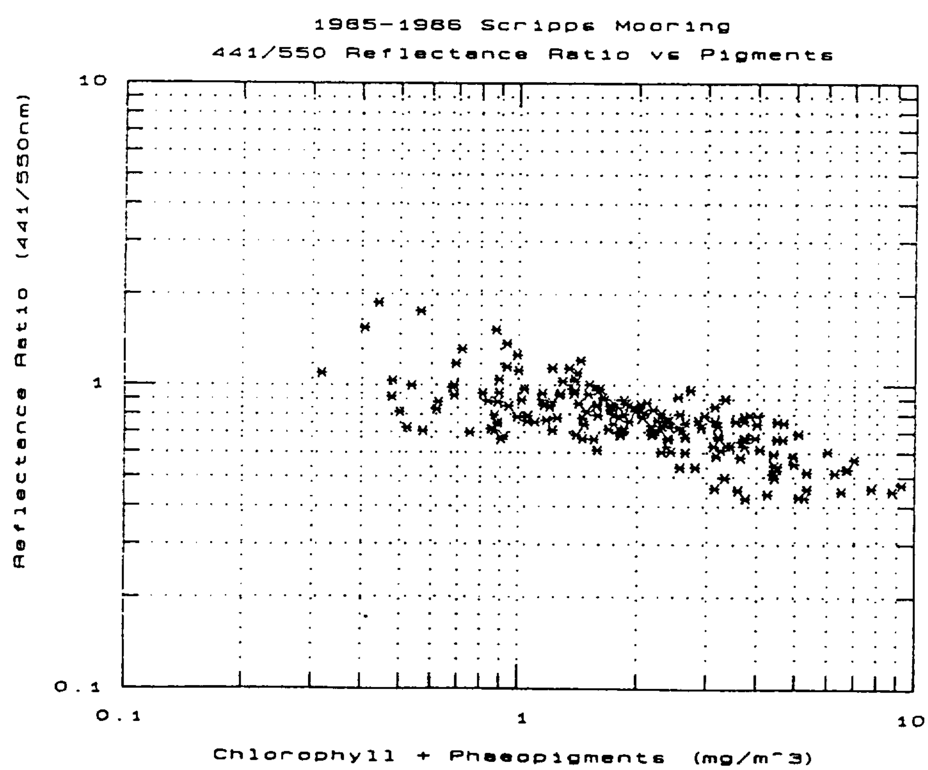

Figure 3b. 441/550 Reflectance Ratio versus Total Pigments during October 85 to May 86.

III. Data Set Example: March 21, 1986

Nearly 300 days of mooring data have been collected from the various moorings involved in this project. It would not be practical to present all of the resulting data. For the purposes of this report we will present selected data.

March 21, 1986 has been chosen as an example day because it was almost cloudless, the platform was in good shape having been recently serviced by SCUBA divers, and skiff based vertical profiling occurred. Figure 4a shows the downwelling irradiance plotted as a function of time from sunrise to sunset at selected wavelengths. As one would expect, this is dominated by the elevation of the sun and the possible presence of clouds. In an effort to look for second order effects, we chose to first normalize the downwelling light field throughout the day to the intensity at a selected wavelength (550nm). A second stage of normalization then normalized every wavelegth to its value at local apparent noon. This enabled us to display the downwelling light field as a surface that was level at noon constant at 550nm. Figure 4b shows the same days data as plotted in figure 4a. Wavelengths longer than 589nm show a steadily varying character reaching a peak in mid-afternoon. Figure 6b, a plot of platform depth, shows the same feature, suggesting that we are seeing the effects of the path of light from the surface to the instrument changing with the tide. This path change will affect parts of the spectrum with larger diffuse attenuation coefficients (red) to a greater extent than the more transparent parts (blue). Another noticeable feature is the more "rough" part in the blue (410,441, and 488nm). This suggests that the attenuation coefficient here is covary with the physical (and presumably biological) constituents of the water column. In later figures we will explore this possibility.

In examining this variability, let's look first at the physical properties during this period. The next figures show certain parameters including (5a) salinity showing a transition at around 12:30 hours from 33.05 to 32.8 parts per thousand (ppt) followed by an upward transient at about 1400 hours and an uptrend starting around 1600 hours. Figure 5b shows temperature as recorded at the platform. This temperature structure mirrors the salinity features in the preceding figure. It is interesting to note that the range of temperature at the platform was almost 2°C during this sunrise to sunset period.

Figure 6a shows a linear plot of PAR (Photosynthetically Active Radiation) at the platform as a function of time along with the calculated solar zenith angle. The relatively smooth shape of the PAR curve indicates that the sky conditions were clear. The next figure (6b) is important because it shows that the depth of the platform does not remain constant or level during the day. The sinusodal depth (pressure) curve reaches a minimum depth during low tide. The sea structure on which the platform was attached has a dynamic nature and the resulting movement is a function of both tide and current magnitude and direction. This dynamic nature results in a modulation of the angle of the platform. Figure 6d shows that the average angle from level of the platform can change by more than 4 degrees due to these effects. It is also important

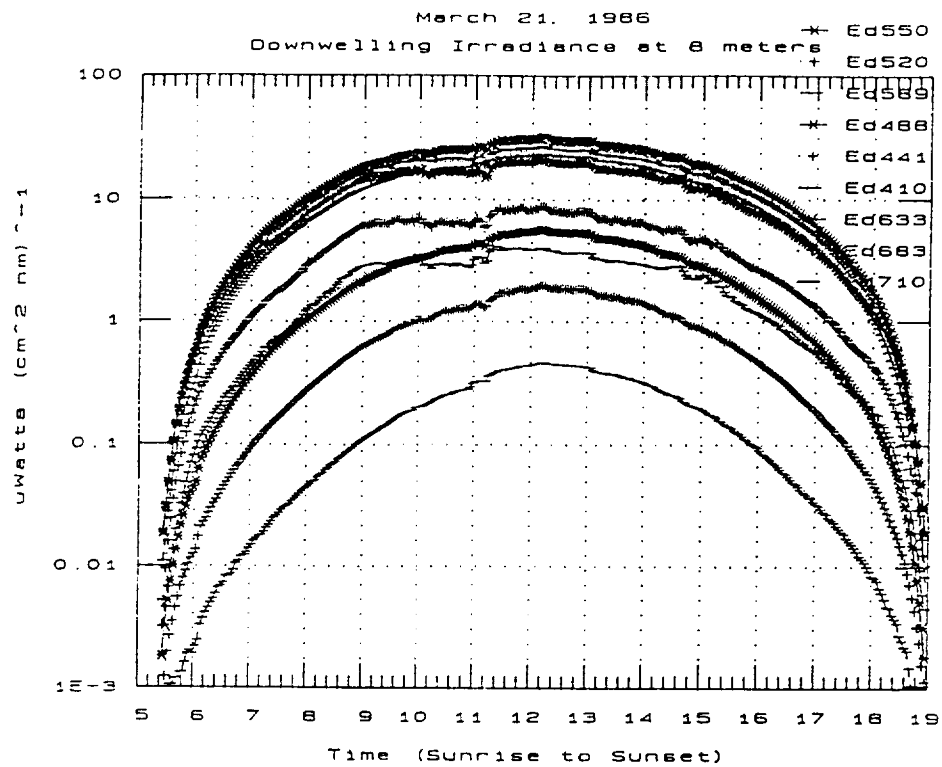

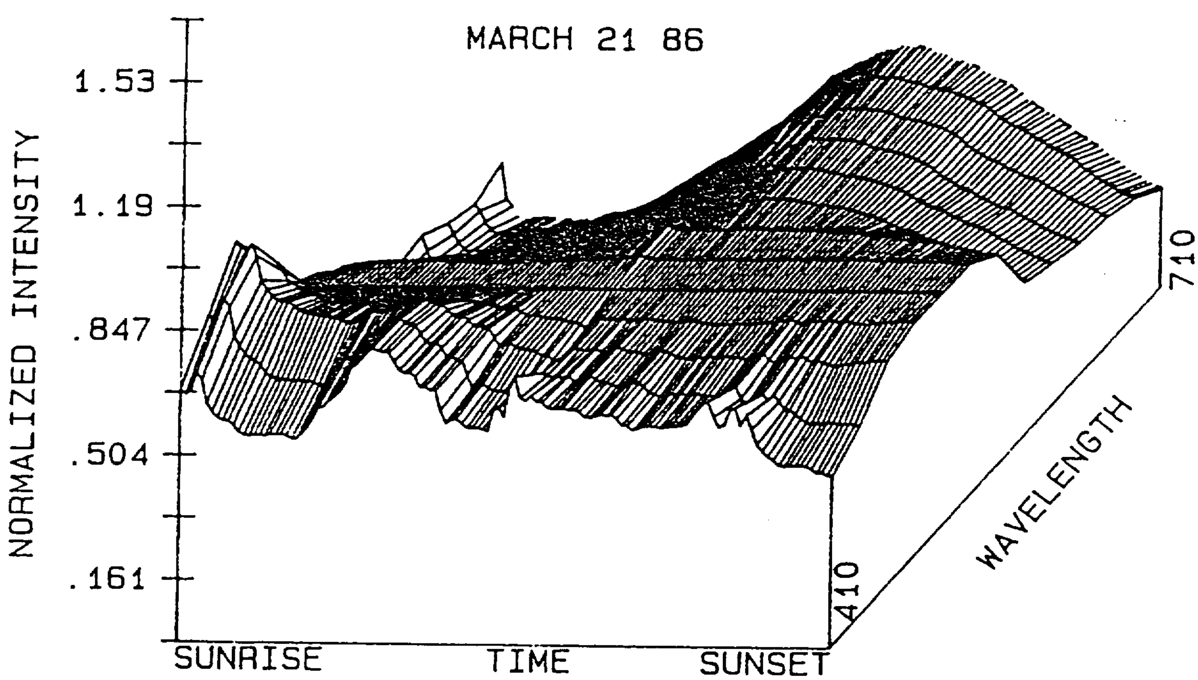

Figure 4. March 21, 1986 Sunrise to sunset mooring downwelling irradiance a. Plot of absolute intensity versus time. b. Normalized to intensity at 550nm and at local apparent noon.

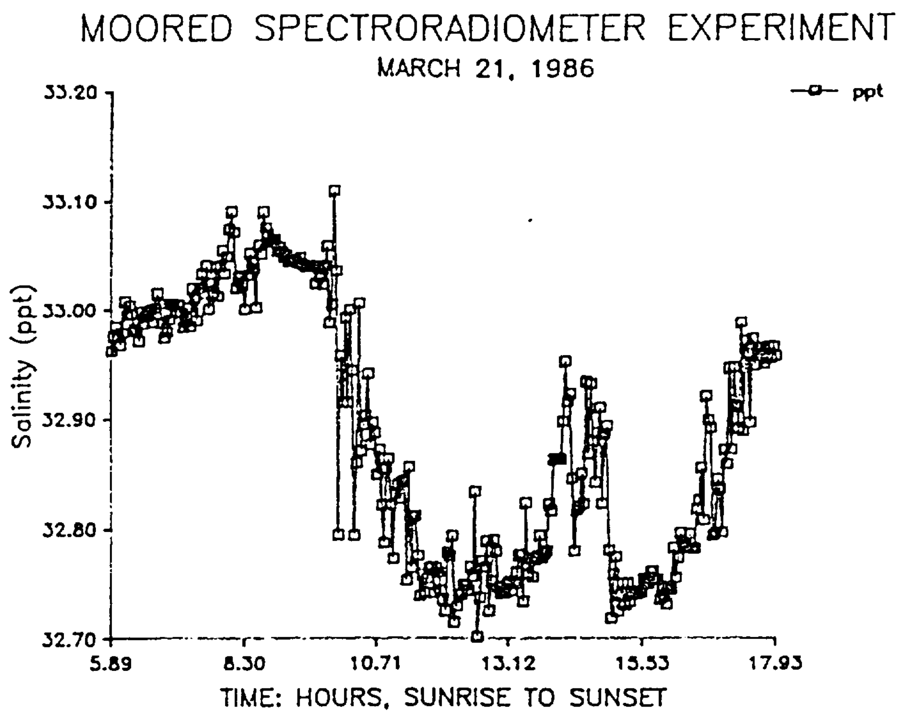

Figure 5a. March 21, 1986 physical parameters: salinity

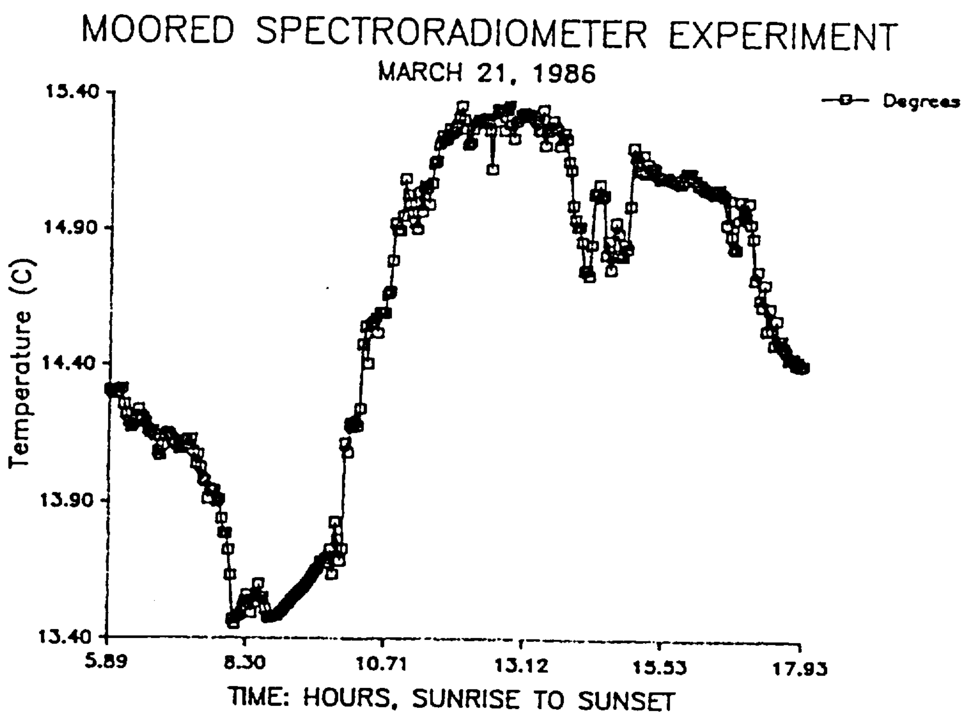

Figure 5b. March 21, 1986 physical parameters: temperature

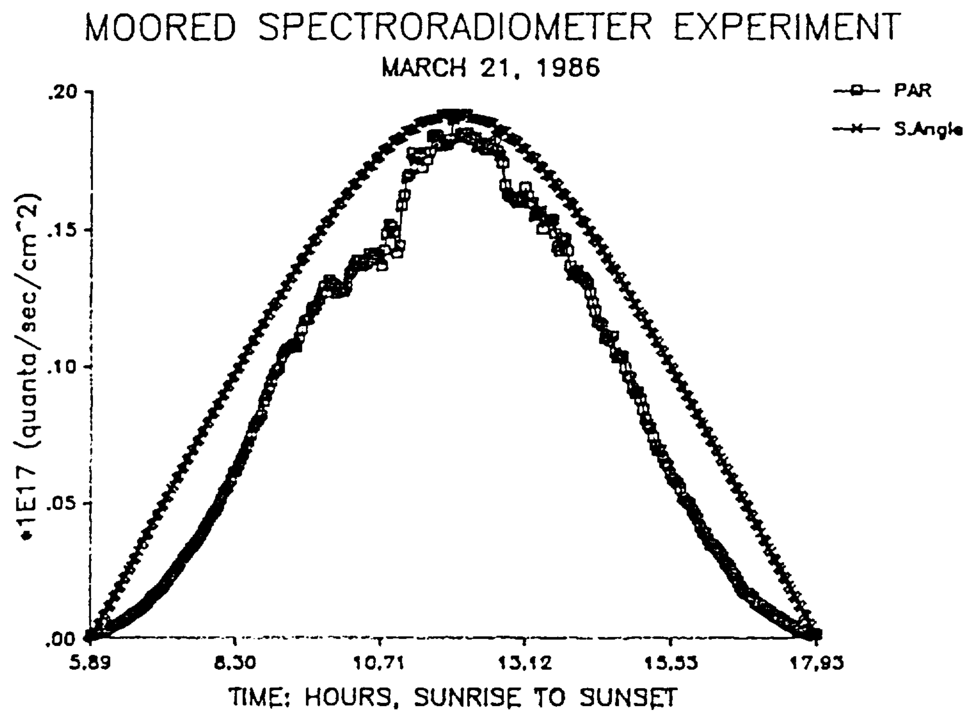

Figure 6a: PAR and sun zenith angle from sunrise to sunset at platform

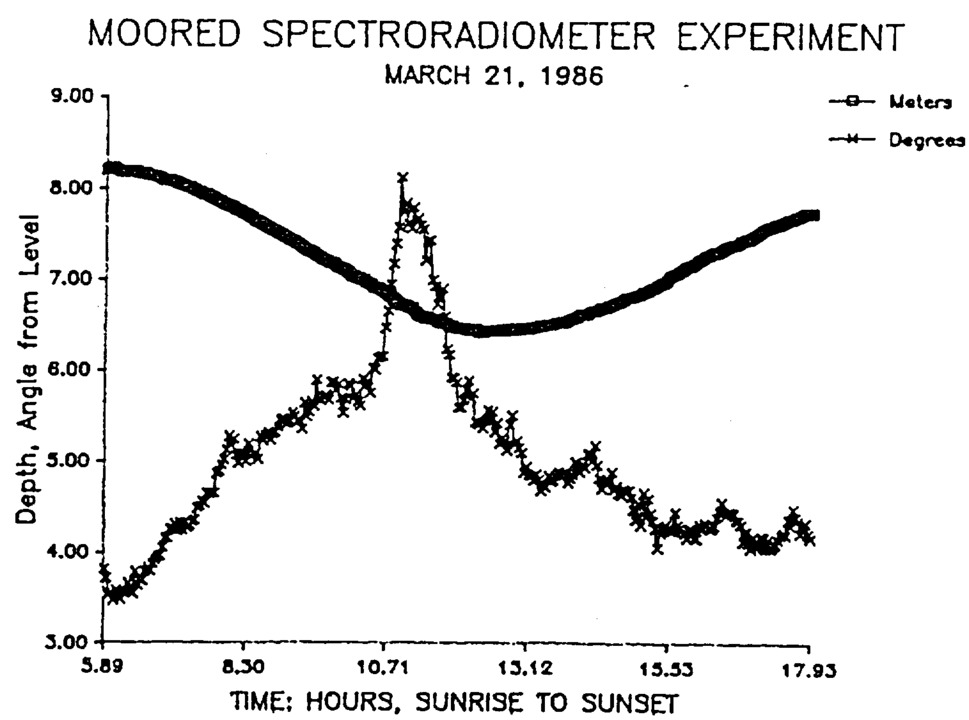

Figure 6b: Average depth below surface and average platform angle from level

to remember that this is the average angle from level and that surface gravity waves induce considerable motion in such a near surface mooring. In a later section of this report we will discuss further the short term attitude of the platform. In figure 4d the angle of the platform is calculated from the "tilt" and "roll" angles of the platform and represents the greatest angle from level in any direction.

Figure 7 illustrates the same day as shown in the previous figure but illustrates some of the parameters that can be drawn from the measurements. Figure 7a shows the irradiance reflectances at two commonly used remote sensing wavelengths: 441 and 550nm. It is interesting to note that 550nm is relatively constant except for transient features in the middle of the day while 441nm reflectance bears a resemblance to the salinity plot in figure 5a. Application of reflectance algorithms developed by Morel in the form

$$C = 1.71 * \left(\frac{R(441)}{R(550)} \right)^{-1.82}$$

have been applied to calculate chlorophyll concentration and are plotted in figure 7b. This equation, R(441) and R(550) are the irradiance reflectances as defined by

$$R(\text{wavelength}) = \frac{E_u(\text{wavelength})}{E_d(\text{wavelength})}.$$

This two-fold change in calculated chlorophyll concentration illustrates the highly variable nature of the Scripps Canyon mooring test site. This is probably due to a combination of advection local upwelling caused by the submarine canyon and tidal flow.

Figures 8a and 8b examine the upwelling radiance at 683. On the 85-86 mooring there were two radiance sensors tuned for 683nm: one was located in the MER in the normal upwelling orientation and the other was located outboard and oriented so that its field of view was 45° out from the shadow created by the moored platform. This was done because it was not known exactly how this shadow would influence the readings. Figure 8a plots the platform angle (in degrees/10) and the ratio (MER/45°sensor) of the radiances from both sensors. The angle plot does not compute absolute angle relative to the same axis as that of the declination of the 45° sensor, but a strong angular dependence is not noted except where the light field becomes very low. At these points, the decrease in this ratio may be caused by either the diffuse nature of the above water light field, the low sun angle, or zero drift on the sensors.

Figure 8b examines the ratio of "Natural Fluorescence" (upwelled radiance at 683nm) to PAR. During the first mooring it became apparent that the upwelled radiances near 683nm were strongly correlated with the chlorophyll concentration. During a related research contract with NASA, we became convinced that this relationship was sound and that the source of this upwelling radiance was almost totally due to chlorophyll

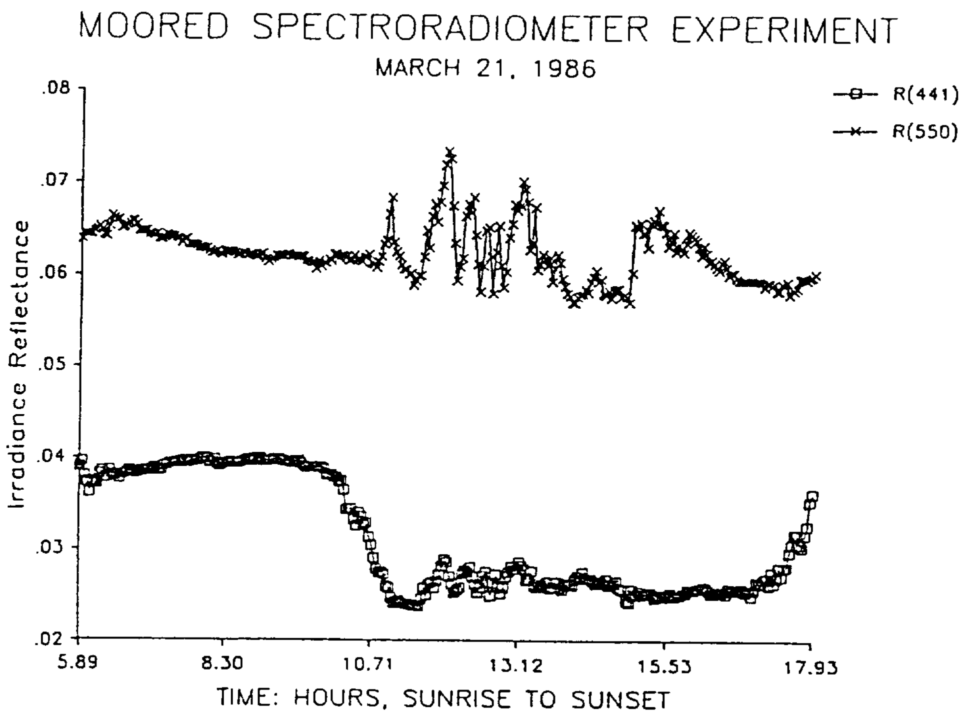

Figure 7a: Reflectance and reflectance ratio at 441 and 550nm

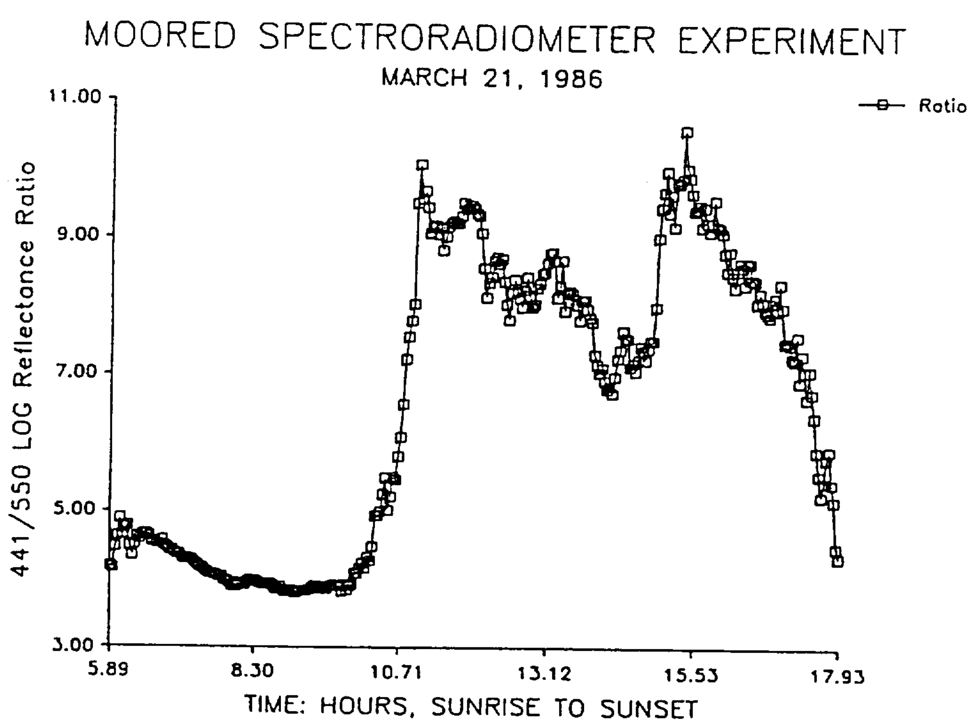

Figure 7b: Reflectance ratio (441 and 550nm) during March 21, 1986

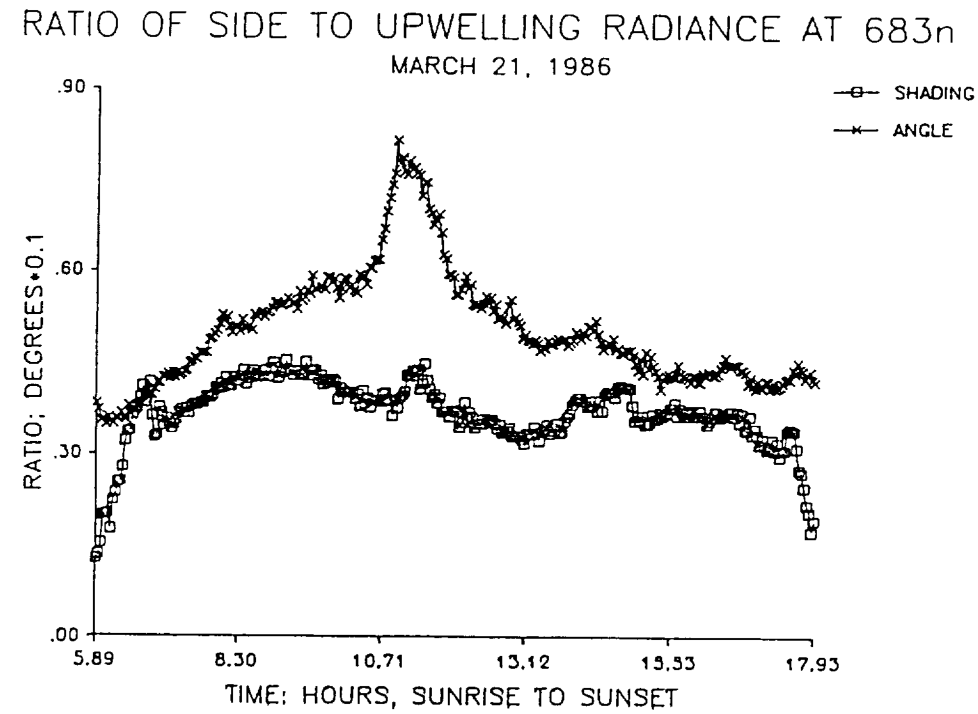

Figure 8a: Upwelling radiance at 683nm: effects of platform shading. The trace labeled "angle" is platform angle (*0.1, degrees) and "shading" is ratio of down-looking to side-looking radiance sensors.

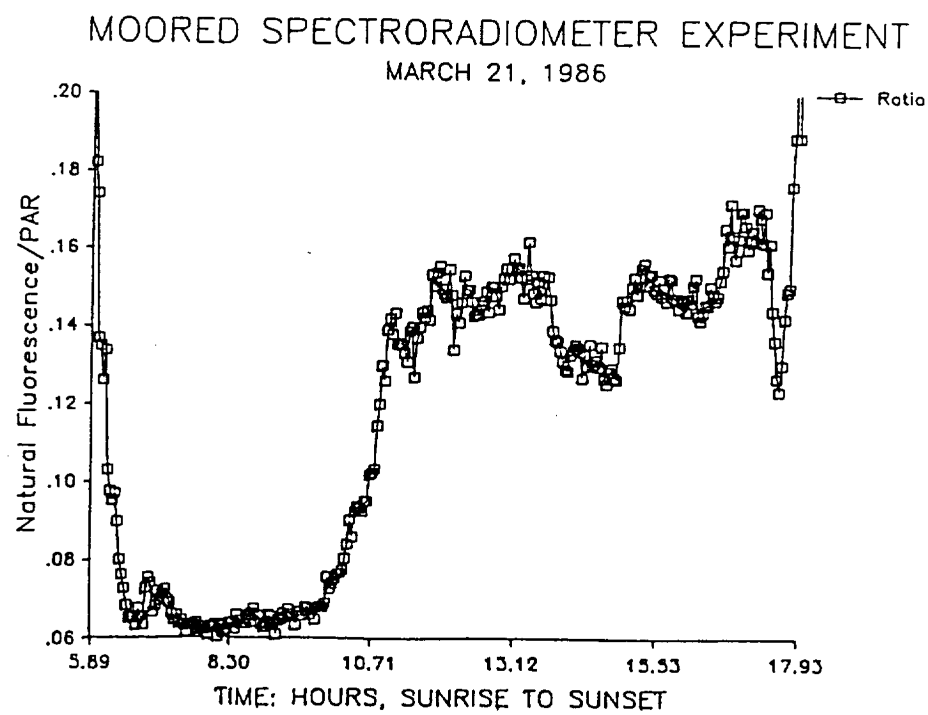

Figure 8b: Natural fluorescence (L_u683)/PAR ratio from platform

fluorescence excited by sunlight (hence the name "natural fluorescence"). Figure 8b shows a plot of this, normalized to PAR. There is a very strong correlation with the plot of calculated (from reflectance) chlorophyll shown in figure 7b.

Figure 9a plots the average cosines at three wavelengths versus time during the same period. The average cosine μ is defined as

$$\mu = \frac{E(\text{wavelength})}{E_o(\text{wavelength})} \quad .$$

E_o is the sum of the upwelling (E_{ou}) and downwelling (E_{od}) scalar irradiances. Of interest in this figure is the ranking of values from high to low: 441,488, and 550nm. It is also interesting to note that it appears that μ_{488} bears the strongest resemblance to the predicted chlorophyll concentration. Further investigations into the significance of μ will be conducted in upcoming research.

Figure 9b displays the downwelling diffuse attenuation coefficients at 441 and 550nm. These parameters were calculated by using data from the two deep irradiance sensors that were suspended below the main instrument platform. They recorded the attenuation coefficient measured over a typical range of 22 meters below the platform. This was effective at recording k, but this k was measured over a range that normally included the thermocline thus including a region of high vertical stratification.

Figure 10a illustrates how variable the Scripps Canyon site can be. This is a plot of every other thermistor in the chain as a function of time. The thermistor were located 3 meters apart with the top sensor approximately 1.5 meters above the platform. The last plot in this series, figure 10b shows the current meter plot versus time. The current meter calibration has not been computed at this time, thus the readings are relative. Both the X and Y axis are plotted.

Figures 11 and 12 were also obtained on the same day between 13:13 and 13:21 hours with the vertical profiling system at a location approximately 100 meters south of the mooring. This location was still in the La Jolla canyon, but avoided possible tangling of the cables from the underwater sea structure. Standard salinity (figure 11a), temperature (figure 11b) and PAR (figure 12a) profiles are shown. A plot of reflectance versus depth may be seen in figure 12b. Unfortunately, the vertical profile was during a period that the mooring was experiencing considerable changes in the reflectance at 550 and in salinity (see previous figures). However, considering this variability, the agreement between the two systems is reasonable.

A plot of the spectral absorption coefficients from vertical profiles on March 21 and May 1 is provided in Figures 13a and 13b. These data were collected according to the methods of Mitchell and Kiefer (1984). Details in the spectral absorption of chlorophyll *a* (435 and 680 nm) phaeopigments (415 nm) and accessory pigments including chlorophyll *c*

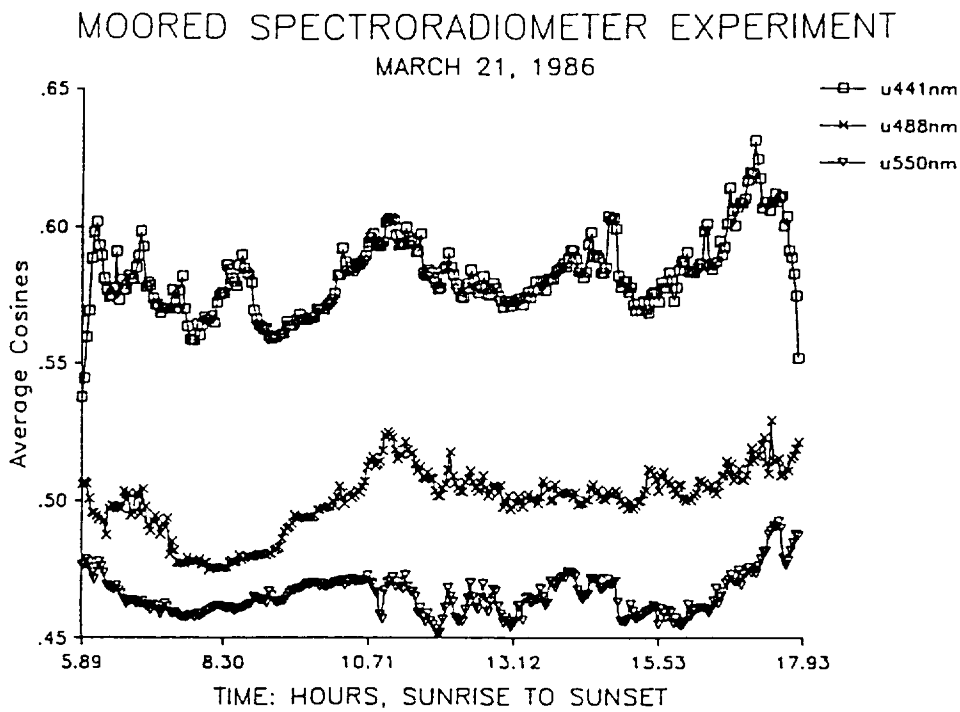

Figure 9a: $\mu(441)$, $\mu(488)$, and $\mu(550)$, March 21, 1986

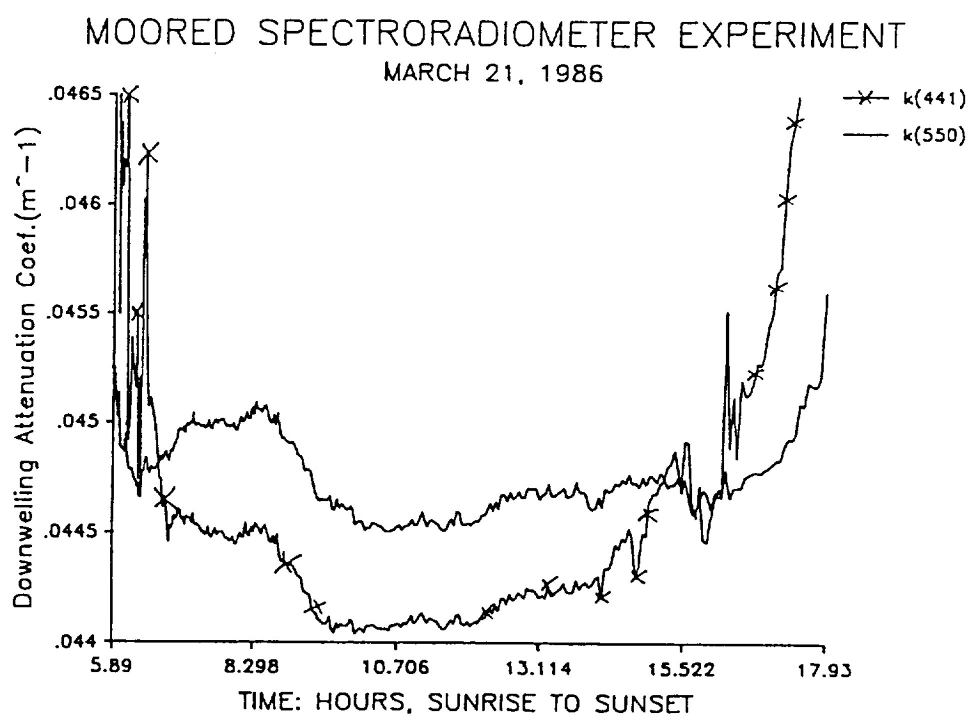

Figure 9b: Attenuation coefficient (441, 550nm) between platform (7 meters) and deep sensors (30 meters) March 21, 1986.

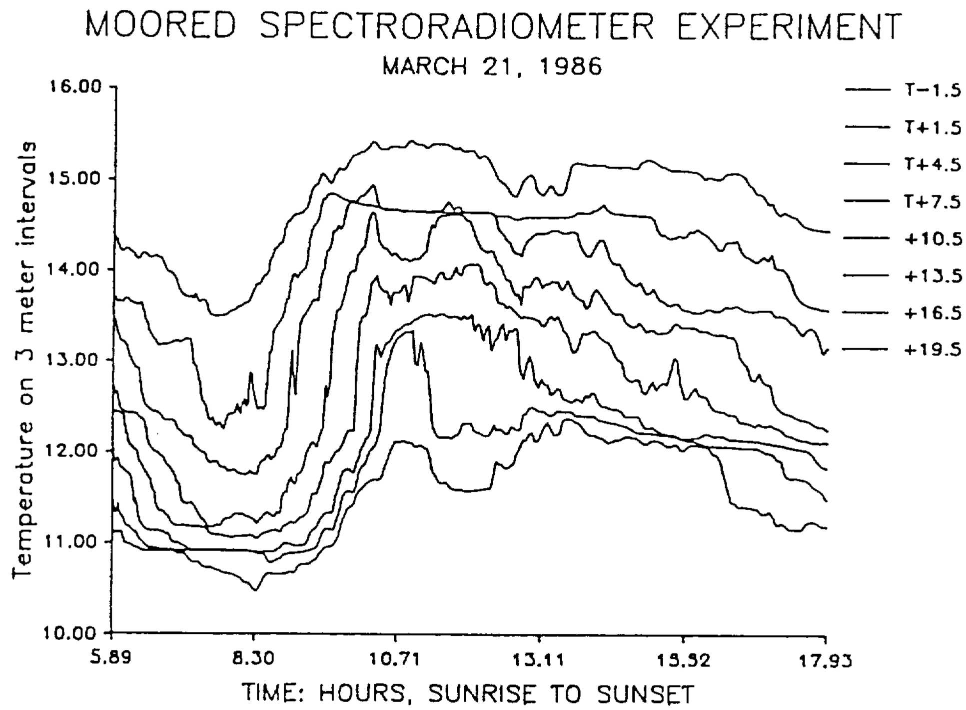

Figure 10a: Thermistor chain data from March 21, 1986. Each element is 3 meters apart starting at approximately 5 meters below the surface.

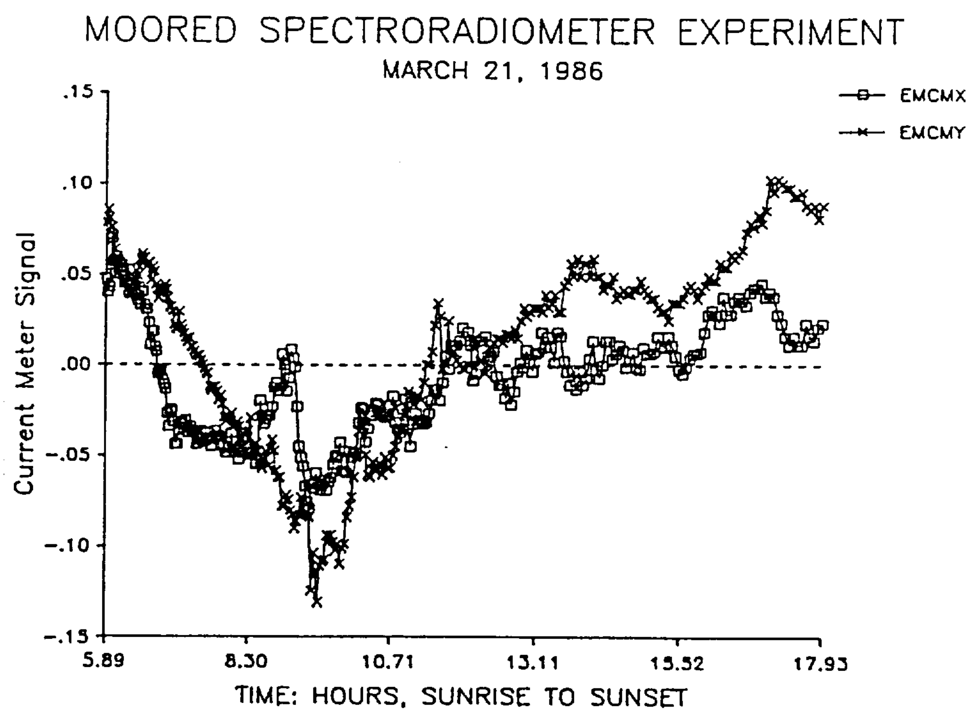

Figure 10b: Current meter (EMCM) at platform during March 21, 1986

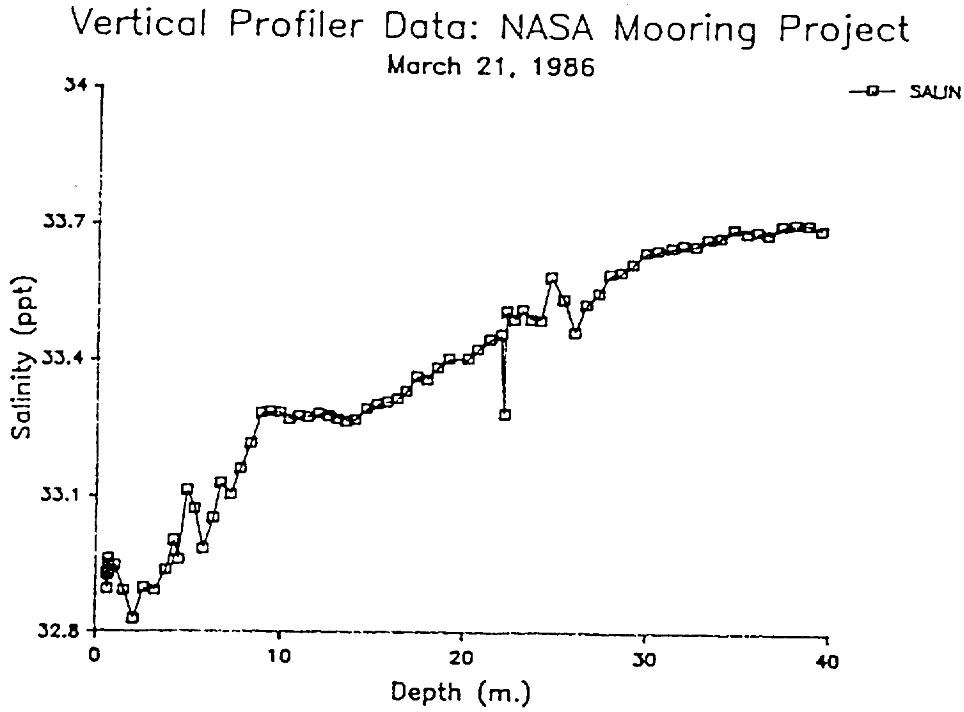

Figure 11a: Salinity profile at site of mooring

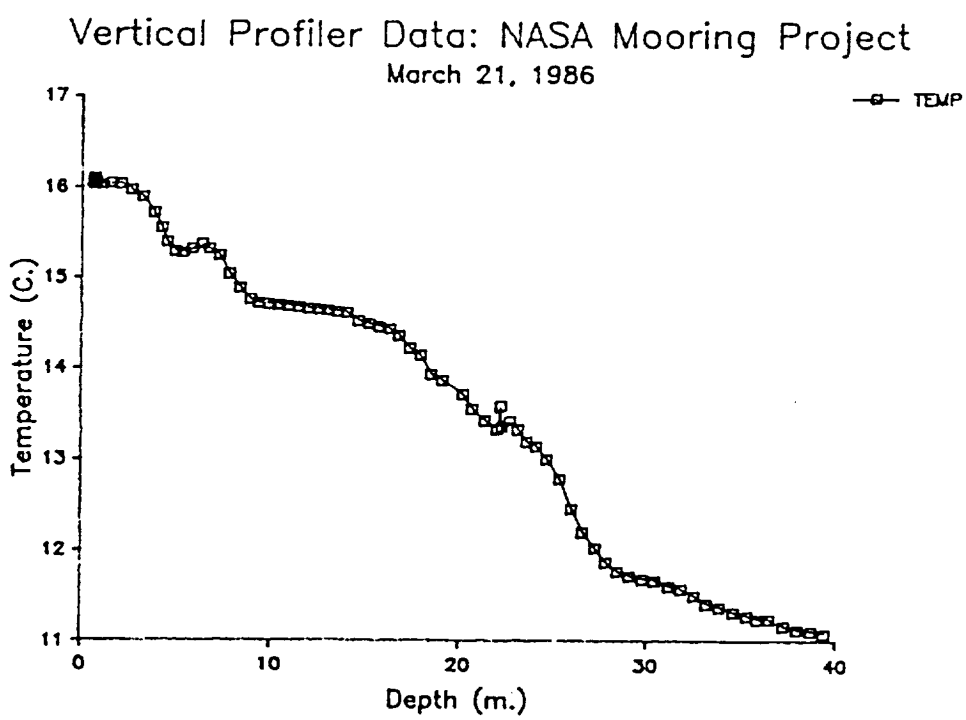

Figure 11b: Temperature profile at site of mooring

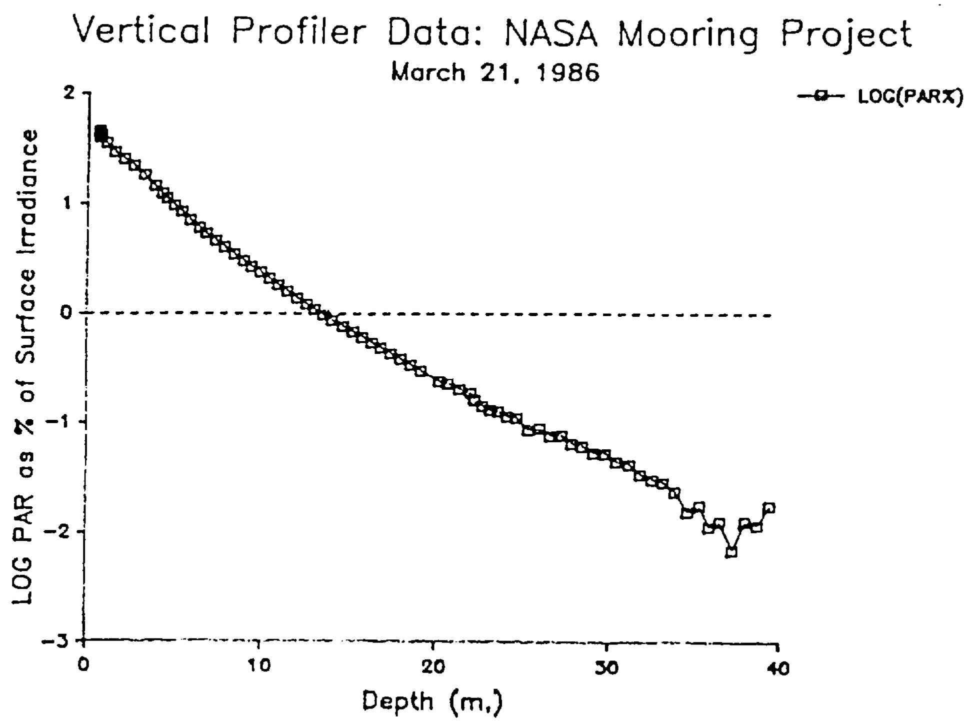

Figure 12a: PAR profile near mooring site on March 21

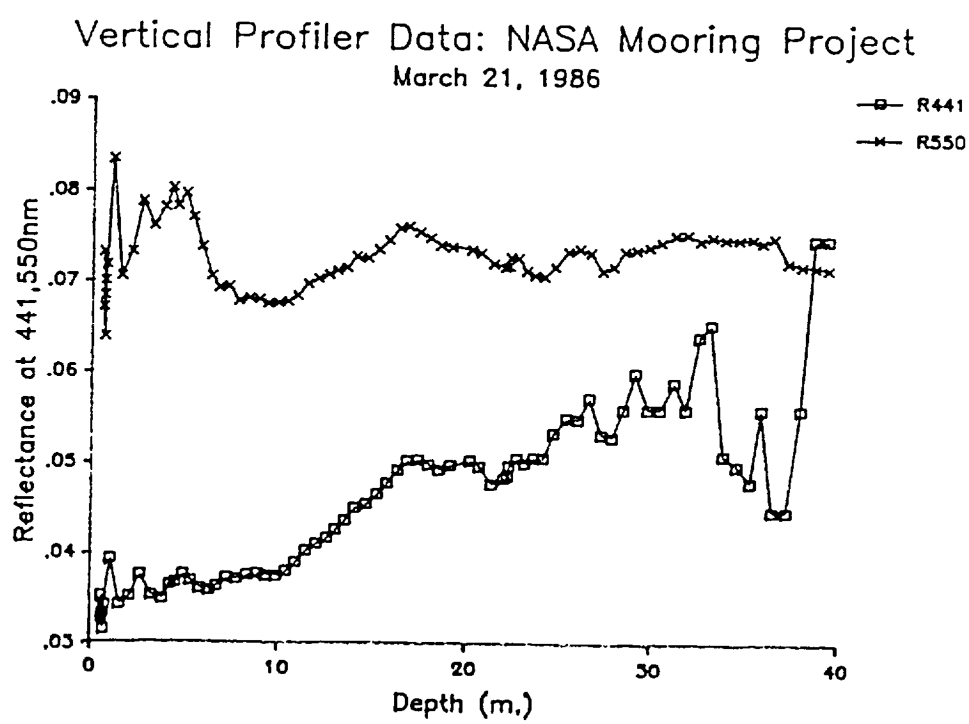

Figure 12b: Reflectance versus depth near the mooring on March 21, 1987

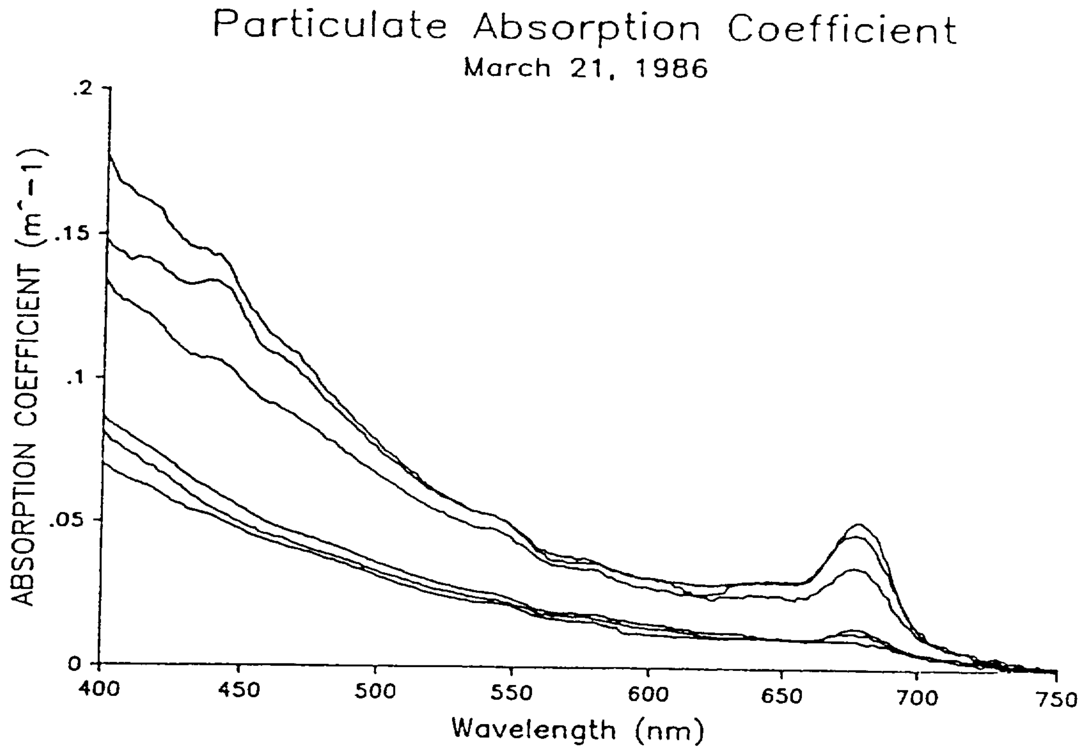

Figure 13a: Spectral absorption coefficients from vertical profile at mooring site on March 21, 1986

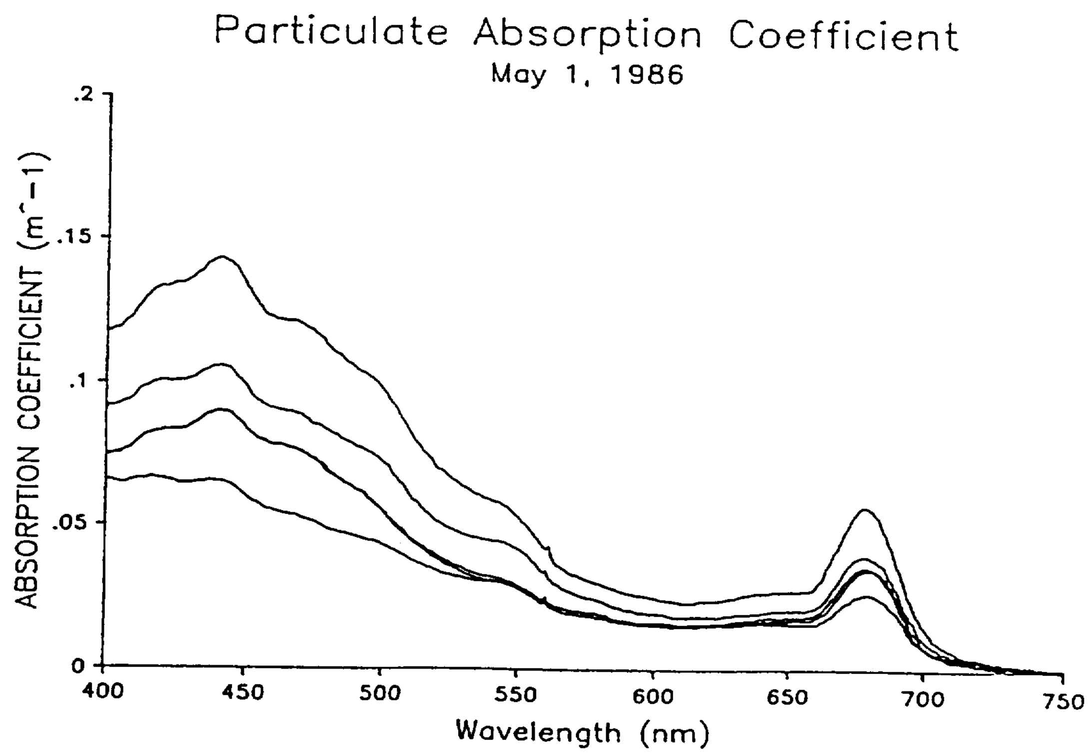

Figure 13b: Spectral absorption coefficients from vertical profile at mooring site on May 1, 1986

(465 nm) carotenoids (470-500 nm) and fucoxanthin (530 nm) are evident in the spectra from May 1. However, on March 21 the spectral structure of particulate absorption is poorly defined, especially in the region from 400 to 600 nm. Total chlorophyll and phaeopigment concentrations were approximately the same on both dates (~5 u/l at the surface). The differences between the two dates are likely due to the relative concentration of detrital pigments. The presence or absence of such pigments pose problems for development of accurate algorithims for the estimation of chlorophyll *a* since variations in particulate absorption dominate the variability in spectral reflectance.

Because many pigments contribute to the particulate optical properties besides the traditionally measured chlorophyll *a* and phaeopigments, modern optical oceanographic studies should include analyses of the pigment assemblage by HPLC techniques (Vernet and Lorenzen, 1987). We determined the concentrations of up to 15 separate phytoplankton pigments by HPLC techniques for 20 separate vertical profiles. We also determined phycoerythrin concentrations using a newly developed technique (Stewart and Farmer 1984, Vernet et al., 1986). A summary of the vertical distributions of 5 of the more important pigments observed on March 21 are included in Figure 14a. Besides chlorophyll *a* and phaeopigments, cyanobacteria specific phycoerythrin, diatom specific fucoxanthin, and dinoflagellate specific peridinin were found to be abundant. It is interesting to note that the peridinin concentration drops off more rapidly with depth than does fucoxanthin, suggesting that the dinoflagellates are concentrated at the surface, perhaps by motility.

Figure 14b illustrates the vertical distribution of primary production and nitrate on March 21. On this date, a moderate bloom was present with highest concentrations of pigment biomass and production occuring at the surface. Nutrients were depleted to low levels in the surface waters. Phytoplankton growth was limited by low light levels below 15 m so that nutrient levels in the deeper water were not depleted.

Study of the temporal properties of the underwater light field is of interest for several reasons. Several studies have been conducted addressing the effects of varying light on plankton growth. Photosynthetic rates were found to increase under fluctuating light by Marra and Heinemann (1982). Abbott and others (1982) reported changes in the fluorescence of chlorophyll during changes in the light field caused by cloud coverage changes.

The following is a discussion of investigations into the time dependence of the optical properties mentioned above (as a function of time on the scale of seconds). During both Scripps Canyon moorings sampling was conducted over a variety of averaging intervals. During the second mooring, data such as that presented above, represents 2048 complete spectral scans averaged over 130 seconds. At certain times during the mooring, the averaging was reduced to increase the sampling rate to one every 0.4 seconds. This enabled us to examine the time dependence of the optical signals on order to best design the time related modes of data acquisition for the moored spectroradiometer under development.

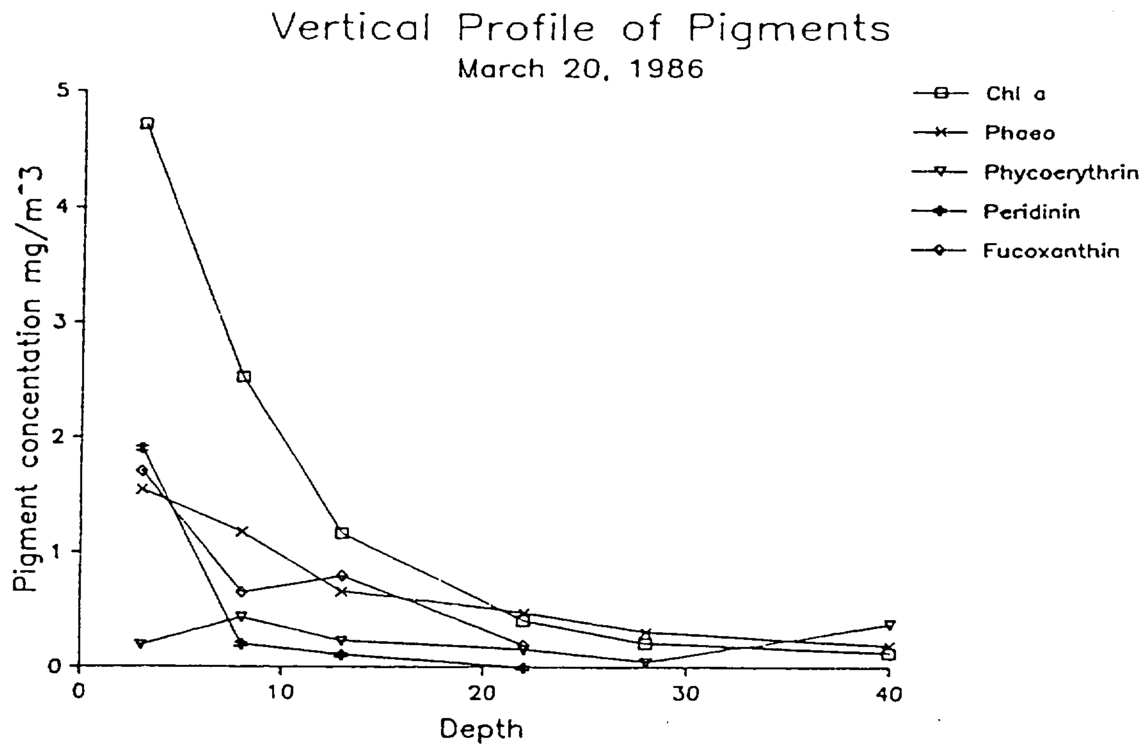

Figure 14a: Vertical profile of pigments from March 20, 1986

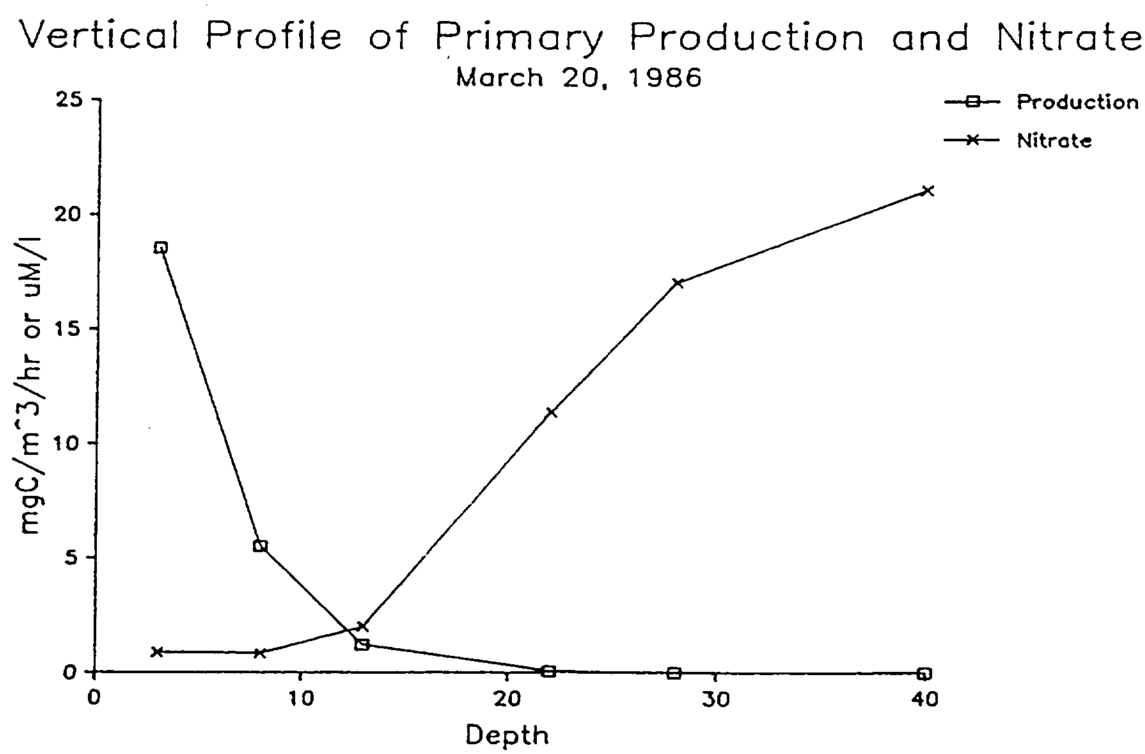

Figure 14b: Vertical profile of production and nitrate on March 20, 1986

In an analogous way to figure 3, we have generated a "surface" plot to show the short term properties of downwelling irradiance. Figure 15 shows a plot of downwelling irradiance with each wavelength normalized to its mean value throughout the observation period. The interesting feature to note is that the amount of variation is greatest where the attenuation coefficient is the greatest. This is to be expected according to the Lambert-Beers law, and the related definition of the attenuation coefficient K_d for downwelling irradiance E_d:

$$K_d(z) = \frac{-1}{E_d(z)} \left(\frac{dE_d(z)}{dz} \right) .$$

From a time series at a single point in the ocean, significant values of *dz* can be obtained from 1) vertical path length changes caused by gravity waves, 2) refractive focusing of light due to waves causing a lengthening of the average path, and 3) changes in sun angle. We feel that this is a significant observation because it may yield a method of computing the attenuation coefficient with a series of observations from a **single** moored instrument in the open ocean. As a test of this theory, we plotted the variance in E_d ($E_d(var,w)$) as a function of wavelength w during 500 samples taken over some 20 gravity wave periods. The shape of this plot strongly suggested the shape of the K spectrum. To further test this possible relationship, the ratio of $E_d(var,$ 550nm) to the known K(550) was used to normalize the $E_d(var,w)$ over the rest of w. Now the agreement across the spectrum was very close. The drawback of this approach is that it needs input of a known K at at least one wavelength.

One approach to calculate K from $E_d(var,w)$ was suggested by Rudy Priesendorfer (in personal communication) as follows

$$k(E_d, x) = \frac{E_d(var,w)}{std(x)}$$

where std(x) is the standard deviation of the wave height. Figure 16b applies this proposed relationship as measured at the mooring and it can be compared with actual measurements of K (surface to 8 meters) from the vertical profiler. Std(x) was estimated from the pressure tranducer located at the platform (8 meters) which underestimates the wave height. Thus std(x) is underestimated. On the other hand, this formula does not account for refractive changes in the underwater light field and these refractive changes may account for most of the variance in E_d. While we have not come to a resolution of this problem and the discrepancies between figures 16a and 16b, their resemblance in shape is remarkable. Accordingly, the newly developed MER-2020 spectroradiometers can also be enabled to record $E_d(var)$.

Figure 17a plots absolute values of downwelling irradiance (441,488,550nm) during 100 seconds in the middle of the day on March 20, 1986. Figure 17b displays the absolute values of the downwelling light field at these wavelengths. Figure 18a plots the downwelling distribution functions versus time. Distributions functions (D) are defined as

$$D = \frac{E_{od}(\text{wavelength})}{E_d(\text{wavelength})} .$$

Figure 18a plots the irradiance reflectance R(441,488,550) versus time. It is notable that the irradiance at 441 is significantly lower that the other two wavelengths. The last figure in this series (18b) shows the physical environment during the previous three figures. The physical parameters of note are the pressure (stated in terms of depth) which is related (but not 1:1) to the vertical water path above the instruments, and the platform deviation from level.

On the longer time scale, Baker and Smith (1979) and Kirk (1984) have discussed the effects of sun angle on the "apparent" optical properties, specifically the diffuse attenuation coefficient. Data from these moorings should prove effective in showing both the effects of cloud cover and of sun angle.

Additional issues that can be addressed with these data include comparing methods of measuring above surface irradiance (e.g. E_{od} versus E_d, PAR versus total radiation) in order to estimate below surface photosynthetically active flux.

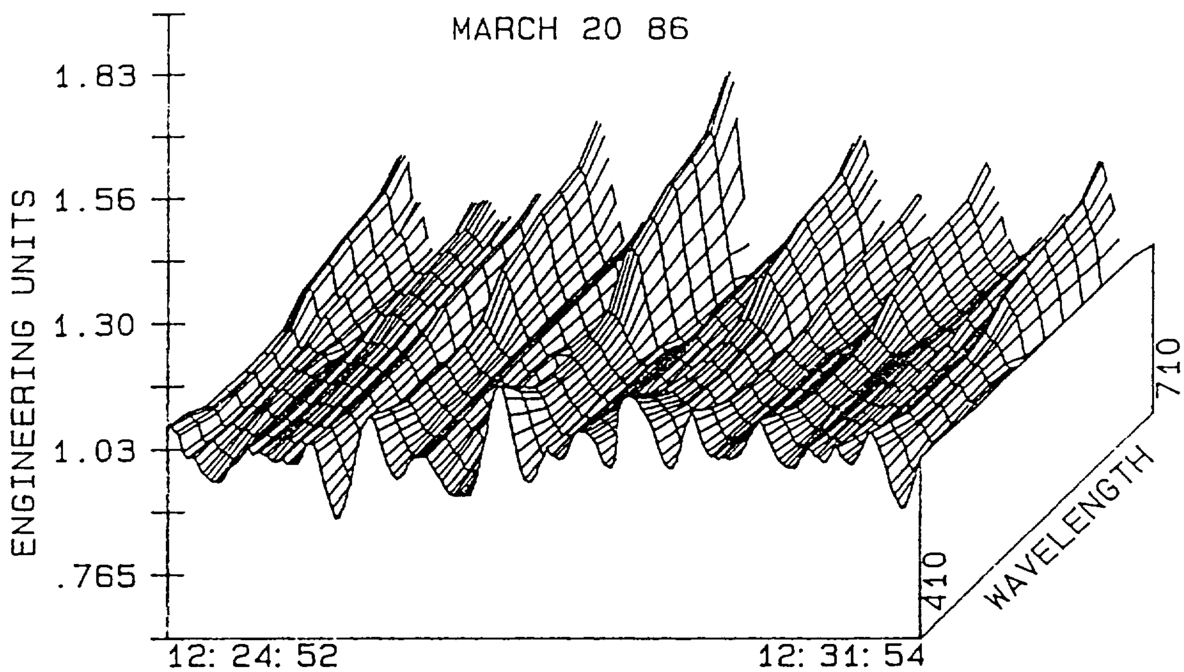

Figure 15: Downwelling irradiance at the platform recorded over 80 seconds. Each wavelength is normalized to its mean value during the series.

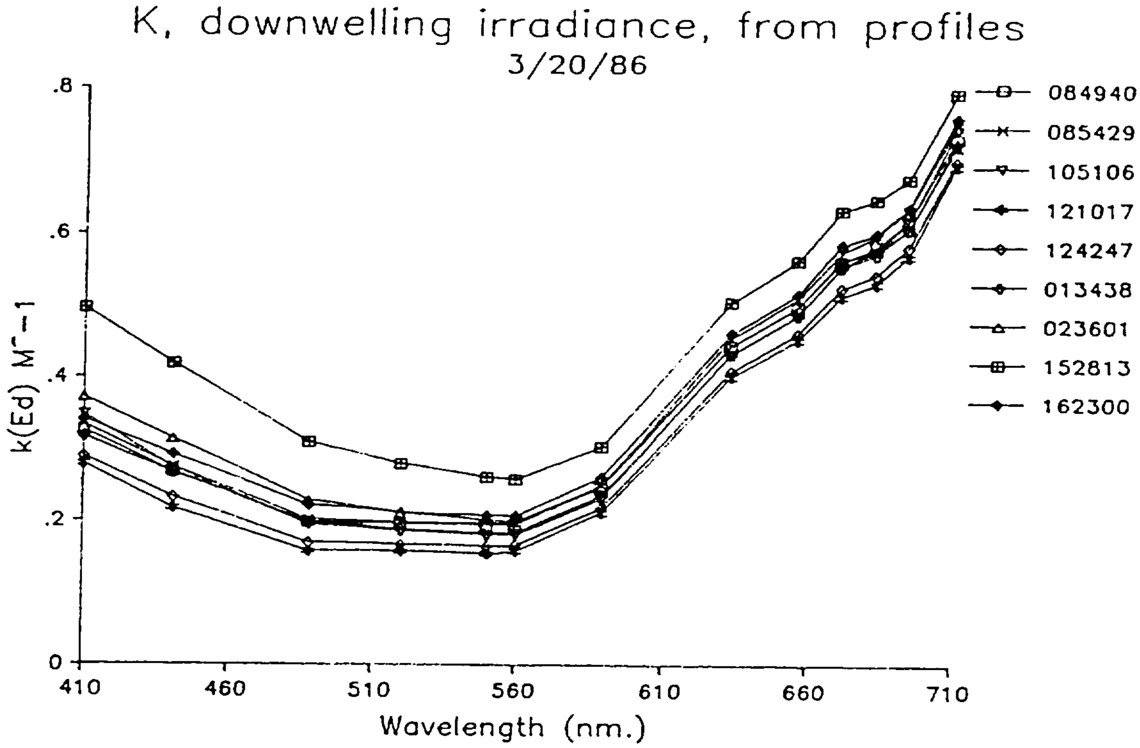

Figure 16a: Downwelling irradiance attenuation coefficient from 0 to 8 meters observed with vertical profiler on March 20, 1986. Time of profile is listed in the legend.

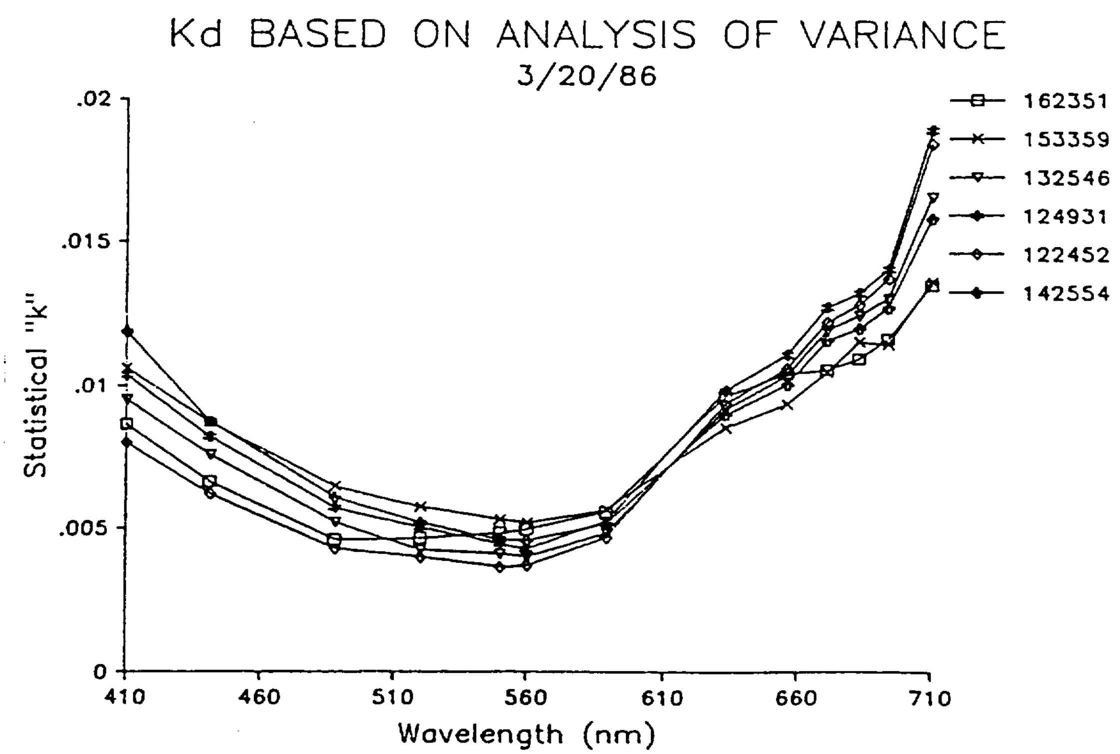

Figure 16b: Calculated irradiance attenuation coefficient from 0 to 8 meters computed from observations of gravity wave caused variance in E_d.

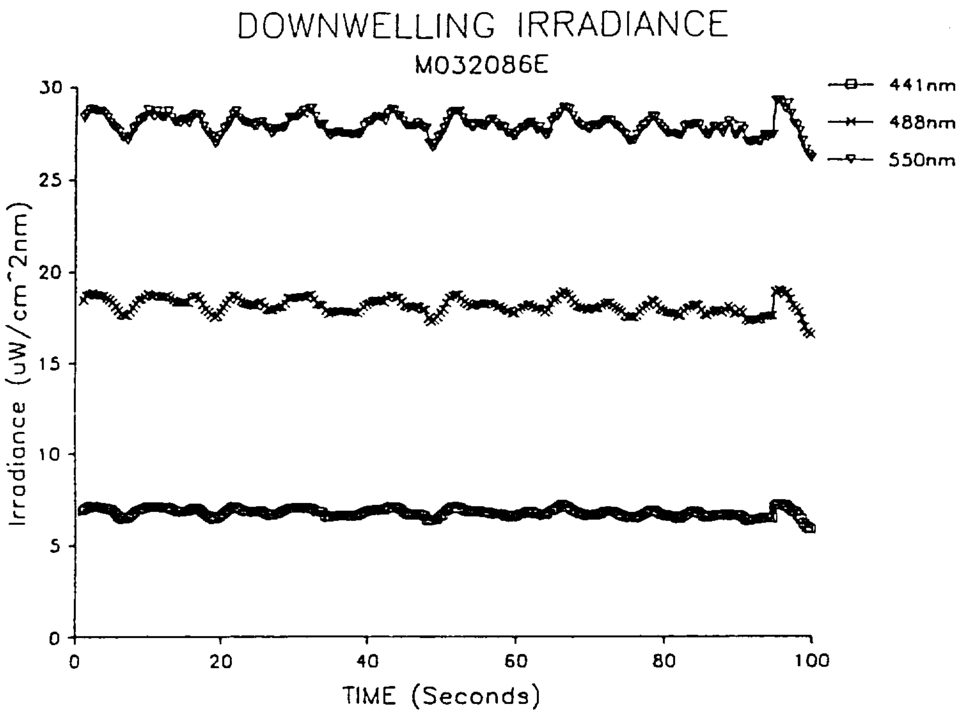

Figure 17a: Downwelling irradiance at 441,488,550nm recorded at a sample rate of 0.4 seconds per sample.

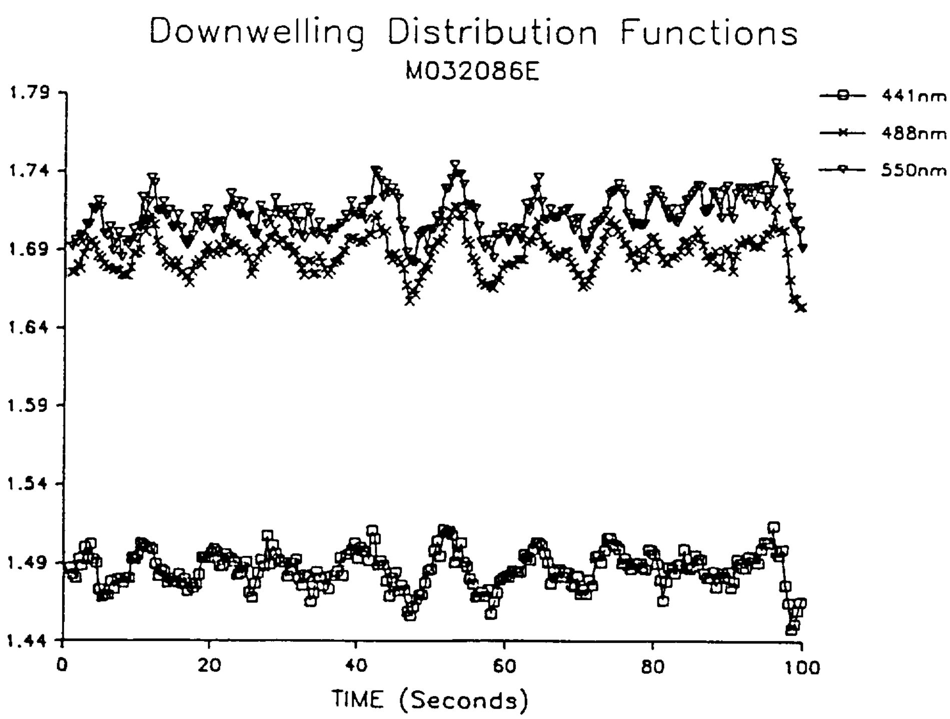

Figure 17b: Distribution functions at 441, 488, 550nm over 100 seconds.

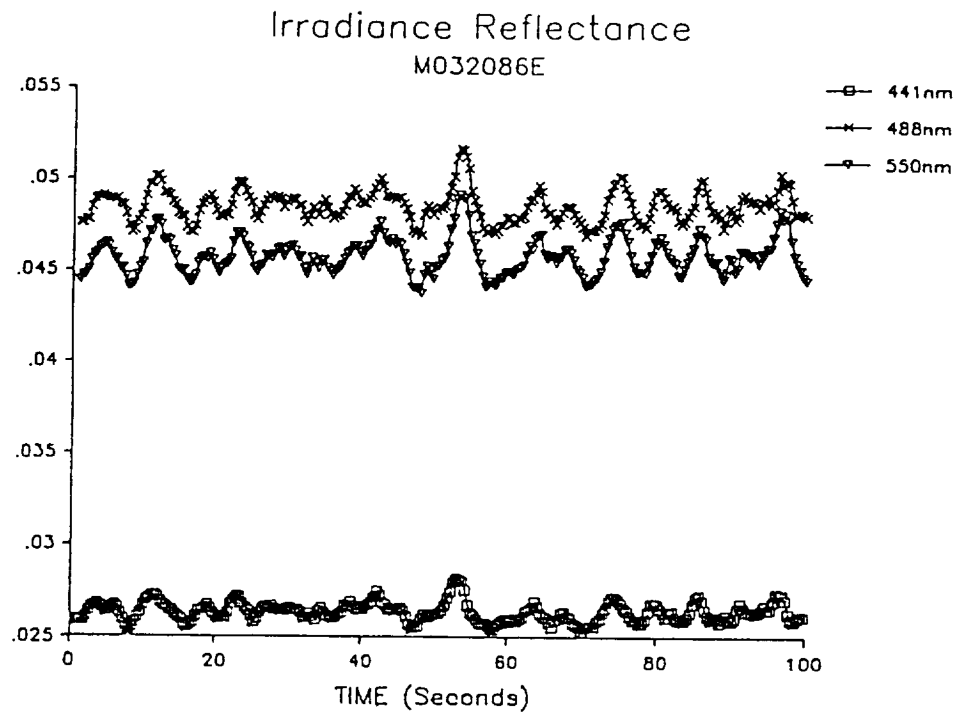

Figure 18a: Irradiance reflectance over 100 seconds at the mooring.

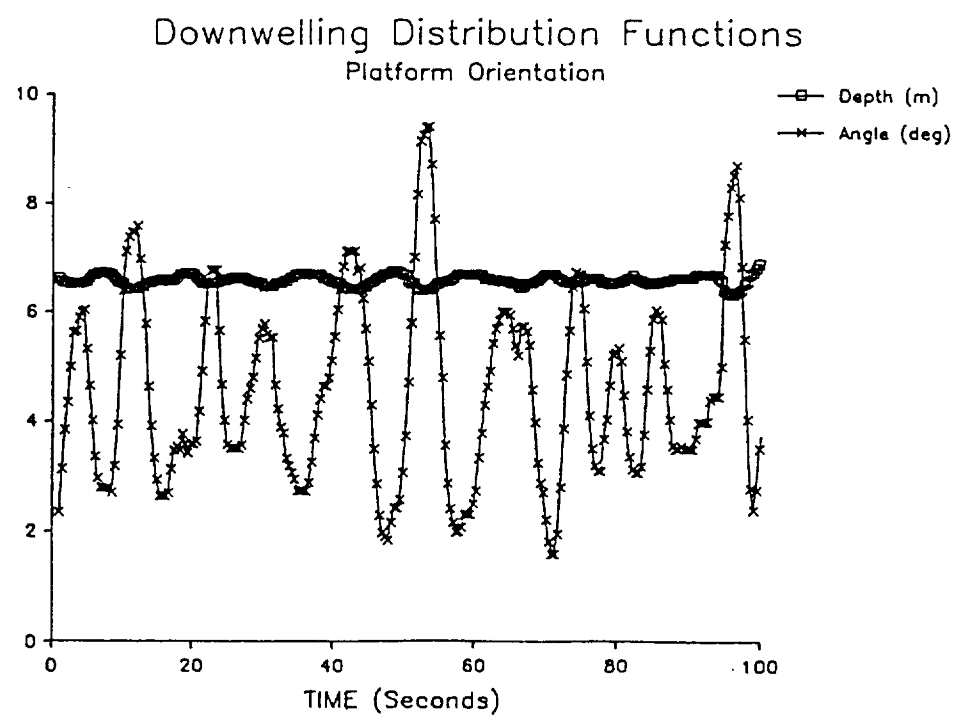

Figure 18b: Platform stability and depth during 100 second sample set shown in previous figures

IV. The MER-2020: Technical Description

The MER-2020 Moorable Reflectance Spectroradiometer is the lead product of this project to design and build a moored spectroradiometer. The MER-2020 features tape storage and both radiance and irradiance arrays. We plan several other models that will be subsets of the MER-2020. The MER-2000, 2010, and 2060 versions use RAM based data storage. The MER-2000 is the lowest cost underwater instrument available in this series. This version features 5 channels of strictly downwelling irradiance. It includes RAM based storage for 15,400 sets of irradiance data without statistics or over 5000 sets with statistics. The model MER-2010 adds the upwelling radiance array. Figure 19 shows a cross sectional view of the MER-2020. Full details of the MER-2020 follow:

Features: MER-2020: Moorable Reflectance Spectroradiometer

* 5 Channels Downwelling Irradiance
* 5 Channels Upwelling Radiance including **Natural Fluorescence**
* 2 axis angle sensors
* Pressure Transducer for depth measurement (200M full scale)
* Battery Voltage, internal temperature, time, date recording
* 448k Bytes of RAM data buffer and **40MegaBytes** tape storage for as many as 400,000 scans of 20 different channels
* Platinum Resistance Temperature Transducer
* Optional Statistical properties (min, max, mean, standard dev.) of the recorded channels

IV A. Sensor Section:

The primary optical sensors used in the MER-2020 series are derived from those featured in the MER-1032 spectroradiometer and are described in the earlier section of this report. Each optical sensor assembly (upwelling radiance and downwelling irradiance) comes standard with five sensors, each sensitive to a different wavelength. The assemblies can easily be expanded to include up to 8 channels of downwelling spectral irradiance, and up to 7 channels of upwelling radiance.

In addition to these optical channels, the instrument can accommodate a variety of additional sensors. A pressure transducer, and two axis housing angle (tilt and roll) are included in the standard instrument. In addition, water temperature is monitored with a platinum resistance sensor mounted on the endplate of the housing. Battery voltage is also recorded.

Optional sensors include the fluorometer and transmissometer manufactured by SeaTech. Future upgrades to the MER-2020 may include interfaces to the series of sensors manufactured by SeaBird Instruments (high speed temperature, conductivity, oxygen), PAR sensors (Biospherical Instruments Inc.), and water current (EMCM).

Biospherical Instruments Inc.

HER-2020 Hoorable Reflectance Spectroradiometer

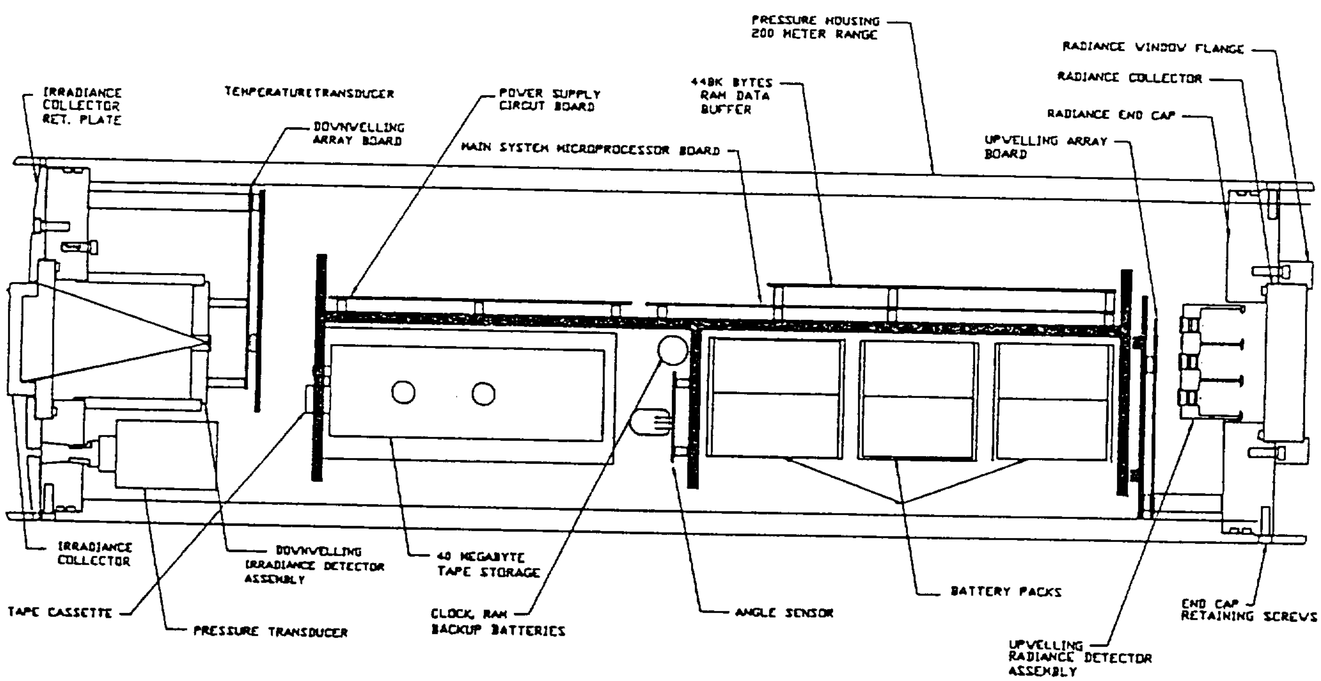

Figure 19. MER-2020 Reflectance Spectroradiometer

IV B. Electronics Section

The electronics section of the MER-2020 is entirely new. The basis of this new instrument family is a CMOS microprocessor (64180) and a 14 bit resolution data acquisition system with programmable gain ranging yielding a dynamic range of over 4 million ($256*2^{14}$). This data acquisition system can address a maximum of 60 analog channels. A block diagram of the MER-2020 is shown in figure 20.

Data retrieval and programming are accomplished via the serial RS-232c interface and a set of programs (included with the instrument) that run on the IBM-PC and "clones". Power is supplied by batteries (not included) which may be alkaline, lithium or lead-acid, depending upon the application. The housing will accommodate a number of different "D" size batteries. For long term deployments (2 or more months), battery packs made up of 9 "D" lithium batteries are recommended. One of these packs will accommodate approximately 2-3 months of sampling,at an averaging time of 60 seconds at 7.5 minute intervals for 14 hours per day. Up to 3 battery packs may be used to allow longer moorings. For short (less than 1 month) mooring periods, alkaline batteries are recommended. Separate user replacable lithium batteries are provided to power the clock and "wakeup" circuitry, and for program and data storage.

IV C. Software Support

The MER-2020 can be configured in a variety of ways, to achieve the desired sampling strategy. These options are selected by sending a binary programming stream of 128 bytes to the MER-2020. The selected options include: The number of readings to average per each data frame stored, the mode of storage (with or without statistics), the time between cycles, the condition of an 8 bit output port provided for control purposes and the number of times to execute before choosing a new sampling mode. "Slots" for three different user definable programs are provided. Three predefined programs are also available, including a "default" program.

A software program written in Microsoft "QuickBasic" (IBM-PC compatible) is provided to aid in programming the MER-2020, and in data retrieval. The source code is provided so the user can customize the software to suit their specific applications. A number of other programs for the analysis of moored optical data are currently being developed. Please consult Biospherical Instruments for availability.

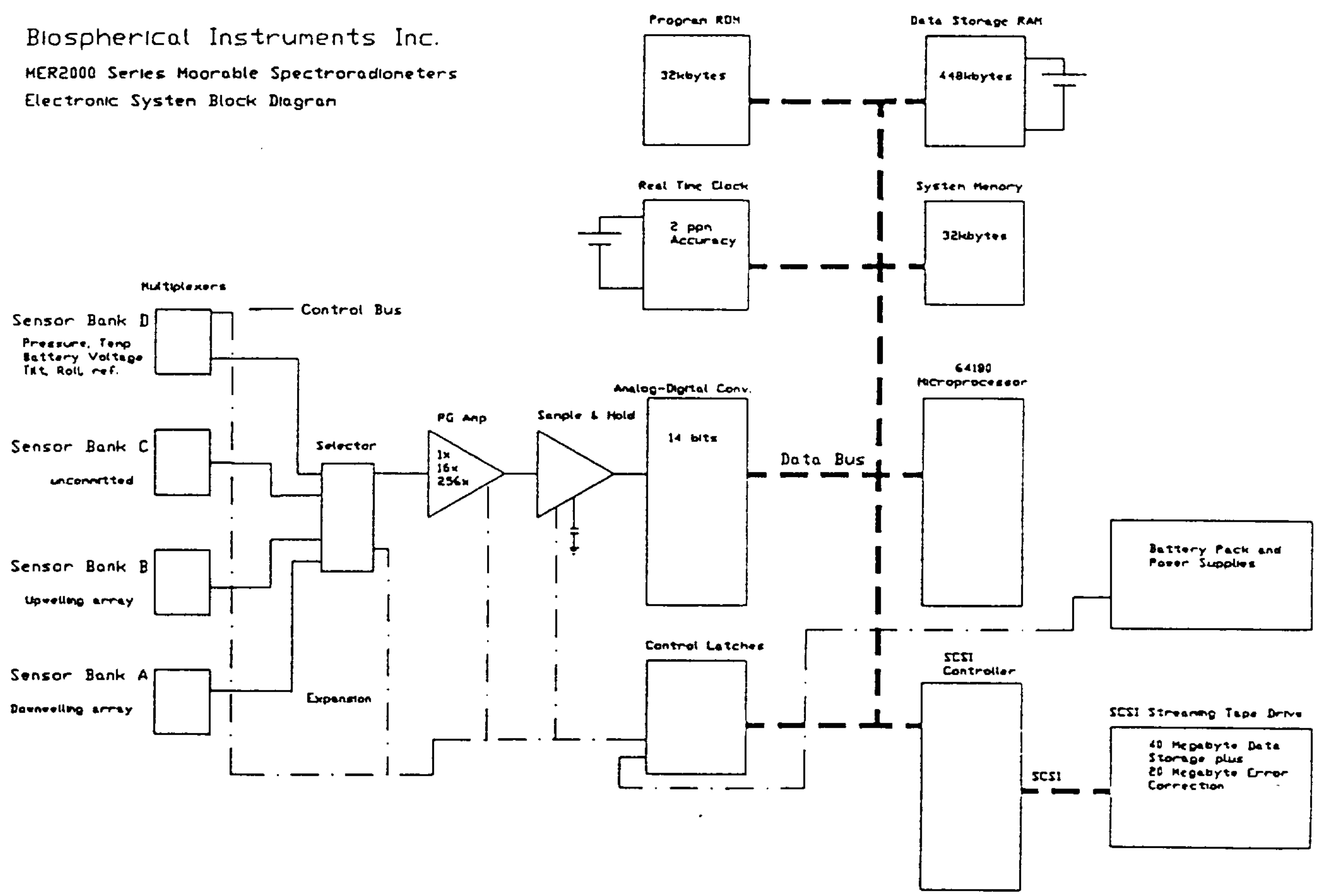

Figure 20. MER-2020 Block Diagram of Electronics Section

IV D. Instrument Housing

The housing for the MER-2020 is hardcoat anodized 6061-T6 aluminum, 8" nominal diameter, 28" long, and of a non-welded design with double o-ring seals. The housing is designed for deployment to 500 meters depth. The standard pressure transducer will limit deployment depth to 200 meters. An optional 500 meter pressure transducer is available for extended operation. Deployment of the instrument will require a mounting frame. Biospherical Instruments can provide these frames or provide you with guidance in their design. The specific design will vary depending upon any external sensors used.

IV E. MER-2020 Data Storage:

Data storage is available in two modes: RAM based and Tape based. The recorded data may also be stored in two formats: Long and Short.

The Tape Drive: The primary data storage device in the MER-2020 is a 40 megabyte tape drive that records on type DC-2000 tapes. The microprocessor controls the tape drive through an SCSI interface on the MER-2020 main board. The tape drive controller communicates with the drive electronics using the QIC36 standard protocol. Tapes are written in the QIC100 format. This format will allow the tape to be read on other devices using this format. Use of the SCSI interface will allow relatively easy substitution of other types of mass storage (e.g. 10 Megabyte "floppy", 80 Megabyte tapes) in the future.

We refer to the tape drive as a 40 megabyte drive, but in fact it is a 60 megabyte drive where 20 megabytes is dedicated to error detection and correction. Data is recorded on 24 tracks with a serpentine pattern on the 205 foot long .25" wide tape. Recording is at 12500 flux reversals per inch (FRPI) using group code recording (GCR). Manufacturers specifications for this tape and drive quote less than one error in 10^{12} bits for verified tapes.

Data Formats: LONG FORMAT: Long format means that the data will be stored with the full statistical information: mean, standard deviation squared, minimum and maximum. The space required for each scan will depend on the number of channels scanned (nc) and can be computed as followed:

$$\text{bytes per scan} = 9 + (16 * nc)$$

Thus if the instrument has 5 channels of downwelling irradiance, 5 channels of upwelling radiance, and 8 channels enabled in the auxiliary multiplexer, (9 + (18 * 16)) 297 bytes of data storage will be consumed per scan cycle.

The RAM data storage area is divided into 8k blocks. Only whole blocks of data will be stored in each block. This means that there usually will be a small amount of space left unused in each block. Using the example of the previous paragraph, 27 complete scan sets can be stored in the 8k (actually 8192 bytes) RAM block. There are 56 blocks available in the RAM for data storage. This means that 1,512 scans can be recorded before the tape drive is used to store data.

When the tape drive is turned on, 56 blocks of data will be written. The total capacity of the tape drive depends upon the tape used. The formatting procedure will condition and test each tape and determine how much good space is available for storage. Generally, the format procedure will report at least 4000 blocks available for storage. Thus, for most tapes, 108,000 (4000 * 27) scan sets can be recorded in long format.

This means that over a 6 month deployment, 24 complete scan sets per hour could be recorded if enough battery capacity is provided.

SHORT FORMAT data storage requires less format and only stores the mean of the readings. The space required for each scan will depend on the number of channels scanned (nc) and can be computed as followed:

$$\text{bytes per scan} = 9 + (4 * nc)$$

Thus if the instrument has 5 channels of downwelling irradiance, 5 channels of upwelling radiance, and 8 channels enabled in the auxiliary multiplexer, 81 bytes (9 + (18 * 4)) of data storage will be consumed per scan cycle. Following the same reasoning as for the long format, 101 scans sets can then be recorded per 8k RAM block, and 5,656 scan sets can be recorded per tape write. A total of 404,000 scans sets can be recorded per tape.

F. Power Consumption and Battery Life:

Battery life for the MER-2020 is a function of the number of active channels, number of scans averaged, warm-up time, external sensors, operating temperature, and other parameters. Critical parameters are the current drain of the configuration that you are using. For example, a standard MER-2020 with 5 each up and downwelling channels, plus the normal auxiliary sensors (temperature, pressure, tilt, roll) will draw approximately 56 ma at an input voltage of 32.4 volts. The supplies in the MER-2020 are wide range but do not have constant efficiency over the full 24 to 36 volt operating range. Current drain readings made on a production MER-2020 had the following values with input voltage:

Input Voltage	Current mA
25	49
26	49.7
28	51
30	52
32	53.5
33	60
34	72.3
35	82
36	92.5

From the above table you can see that battery voltage will influence the operating life. The optimum solution is to obtain batteries that can will operate in the 25 to 32 volt region during most of their life.

Power consumption is greatly increased when the tape drive is powered up. The exact power requirements for the tape drive are hard to measure since it is greatly dependent on the mode of operation of the drive. Typical drains range from 370 to 800 mA. There is a turn-on surge of several amps for a few tens of milliseconds.

The tape drive's data-write cycle normally lasts 2.5 minutes. There will be a maximum of around 90 tape write cycles to fill a tape. This means 3.7 hours. If we figure 4 hours at .6 amps, then 2.4 amp-hours of capacity is typically used to fill a tape. This is normally much less than the power requirement to keep the sensors and microprocessor powered on to collect the data.

RAM Backup Battery: The RAM in the MER-2020 is always powered on with its own battery. The normal power drain for this bank of RAM is 5 microamps but may reach several hundred microamps under certain conditions. This battery should be replaced when the voltage is below 2.8 volts or before an extended deployment.

Clock Backup Battery: The clock calendar in the MER-2020 is always powered on with its own battery. The normal power drain for this integrated circuit is 25 microamps (ranging to a high of several hundred microamps under certain conditions). This battery should be replaced when the voltage is below 2.8 volts or before an extended deployment.

IVG. Calibration of the MER-2020:

Optical calibration of the MER-2020 is done in accordance with the methods outlined in NBS Tech Note 594-2 covering the calibration of spectroradiometric instrumentation. Biospherical Instruments uses a Standard of Spectral Irradiance of the "FEL" type. Spectral immersion coefficient corrections are calculated following the procedures of R. C. Smith (1969). These standards are tracable to the National Bureau of Standards.

The pressure calibration of the depth transducer is done hydraulically by comparing the MER reading to that of an absolute pressure transducer calibrated using a "dead weight standard".

IV H. SPECIFICATIONS: STANDARD MER-2020:

OPTICAL SENSORS:

Downwelling Irradiance Channels: 5 standard: 410,441,488,520,560nm. Up to 3 additional channels may be added in the region of 410-710nm to the standard assembly. Custom assemblies of up to 15 channels may be supplied.

Upwelling Radiance Channels: 5 standard: 410,441,488,520,683nm. Up to 2 additional channels may be added in the region of 410-710nm. Custom assemblies of up to 15 channels may be supplied.

DYNAMIC RANGE: 14 bits (16384) with microprocessor set gains of 1, 16, or 256 giving a dynamic range of 1 to 4,194,304.

SENSITIVITY AND NOISE LEVELS:
DOWNWELLING IRRADIANCE CHANNELS ------------------------

Wavelength (nm)	Irradiance (in air)	Irradiance (in water)	Maximum Irradiance	Minimum Signal*
441	168	98	300	.009
488	179	109	300	.006
560	172	97	300	.006

UPWELLING RADIANCE CHANNELS --------------------------

Wavelength (nm)	Downwelling Irradiance (in air)	Upwelling Radiance (in water)	Maximum Radiance	Minimum Signal*
441	180	.66	40	.0002
488	201	1.1	40	.0001
560	183	1.0	40	.0001
683	145	.08	40	.0001

NOTES: Irradiances in microwatts/cm^2/nm, radiances in microwatts/cm^2/nm/str. Upwelling surface measurements are highly variable, these are presented for reference purposes only.
*Minimum signal levels are for 5% resolution and no scan averaging.

SENSOR TIME CONSTANT: Optical sensor response time is typically 0.1 second. Other response times are available for special applications.

IRRADIANCE OPTICAL COLLECTOR: Cosine corrected irradiance diffuser, 2.5" (6.3cm) diameter acrylic plastic collector.(Based on a design by Professor R. C. Smith, documented in the <u>Journal of Marine Research</u>, 27:341-351 (1969).

RADIANCE OPTICAL COLLECTOR, Radiance field of view defined with 7 Gershun Tube elements with anti-reflection baffles. Field of view is 10.2° half angle through Plexiglas window. Details furnished upon request. Oriented to measure upwelling radiance.

BANDWIDTH: 11nm (±3nm) per channel half power bandwidth 0° to 30°C using three cavity interference filters with external blocking filters.

SPECTRAL STABILITY: Less than 2nm shift in 0 to 30 degrees C.

STRAY LIGHT: Typical response (per nm) more than 100 nm outside a sensor's passband is one part per million relative to the peak response. Response more than 200 nm below the passband is typically 0.01 PPM of peak response.

TEMPERATURE COEFFICIENTS: 0 to 30 °C.
ZERO READINGS: Below 0.0002% FS/°C.
RESPONSIVITY: Below 0.05%/°C.

DATA OUTPUT: Serial RS-232c data transmission 9600 baud. Data may be monitored during acquisition at the underwater bulkhead connector.

CALIBRATION: Calibrated at the Calibration Laboratory of Biospherical Instruments Inc. using a type FEL Standard of Spectral Irradiance traceable to the National Bureau of Standards.

DEPTH (PRESSURE) SENSORS: 200 meter full scale. Total error less than 200 meters.

OPERATIONAL DEPTH: 200 meters. On special request, housings to 500 meters are available.

EXTERNAL SENSORS: The MER-2000 series instruments may be connected to various external sensors. The MER-2020 comes with an external connector for interfacing two external sensors such as a transmissometer & fluorometer (XSJ-9-BCR connector). Expansion boards for an additional 8 analog channels are also available.

ADDITIONAL OPTICAL CHANNELS: Additional detectors may be added to bring the instrument to a maximum of 8 downwelling and 7 upwelling channels. Consult factory for the available wavelengths. Expansion to 15 channels or wavelengths is being considered as an option.

IV I. Operation of the MER-2020

Operation of the MER-2020 involves three phases: 1. Installation of batteries and programming of sampling schedule, 2. deployment, and 3. retieval of instrument and data. A brief description of the methods of communicating with and programming the MER-2020 follows.

Communicating with the MER-2020: The user may interact with the MER-2020 on two different levels. The normal level of interaction is through the supplied IBM-PC programs written in QuickBasic. The second level of interaction, called the "monitor mode", is with a standard CRT terminal connected directly to the MER-2020. The first mode operates the MER-2020 in binary format for faster programming, while the second mode utilizes a text oriented menu driven program that is resident in the MER-2020. This second mode is used in trouble shooting and check-out. The first mode is used normally to program the MER-2020 sampling conditions and to dump data.

The MER-2020 is designed to be programmed before deployment and then to start executing a predetermined set of commands ("program") at a set time. Programs may run for a set number of executions, may load in other programs, or may continue executing indefinitely. Parameters under user control include number of channels to sample, number of scans to average for every data set recorded, warm-up time before scanning, number of time to repeat, amount of time between data sets, storage addresses, and others.

There are eight program "slots" available in the MER-2020. The first slot, (0) is where the currently executing program is located. This slot is overwritten whenever a new program is loaded. This is also used for loading a program where only one program is to be executed. Program slots 1-4 are available for user definition. Slots 5, 6, and 7 are defined in ROM and cannot be edited. The have been previously defined for typical operations.

Data storage occurs in two places: RAM and Tape. Normally data is written to RAM. When the available RAM is filled, then a special operational cycle occurs where the tape drive power supplies are turned on, the tape conditioned, and the entire RAM data bank is written to tape. This occurs once per 448k bytes of data. The tape write cycle takes 2-3 minutes to complete and data recording is suppressed during this period.

V: The BIOWATT Mooring: First Operational Deployment

The most important test of a new instrument is a an operational deployment by the first customer. The first customer in this in case was Prof. R. C. Smith of the UC Bio-Optics Group (UCSB), who used the MER-2020 in the BIOWATT project. The BIOWATT program is an interdisiciplinary program supported by the Office of Naval Research. One of its primary objectives is to study the temporal and spatial variability of optical properties and bioluminescence in the open ocean. Funding for the UCSB MER-2020s came from NASA.

The first Biowatt deployment saw MER-2020s deployed at 30 and 50 meters depth. The deployment was a success with full data recovery from the MER-2020s. An additional prototype surface mounted MER-2060 (no tape storage) was deployed at the surface, but there was insufficient space for data storage and due to a programming error by Biospherical, data was lost. The 100% recovery of the MER-2020 was considered a good test.

TABLE VII: MER-2020 Serial Numbers 8702, 8703 data recorded over the period of February 26 to May 4, 1987 at midnight. This represents the noise levels of these two instruments. Data in microwatts/cm²/nm (irradiance) and microwatts/cm²/nm/str (radiance). Note that the data reported below represent the variances, etc, of data that has been previously averaged for 100 scans. This represents the uncertainty in similarly averaged data only. Noise levels on future production instruments in the spectral region of 400-480nm is expected to be lower.

	410Ed	441Ed	488Ed	520Ed	560Ed
			S/N 8702		
mean	4.197e-6	3.676e-6	-2.65e-6	4.423e-6	-6.48e-7
maximum	2.567e-3	4.347e-3	1.561e-3	1.187e-3	5.9e-4
minimum	-2.04e-3	-2.71e-3	-1.61e-3	-1.14e-3	-5.47e-4
variance	1.034e-6	1.771e-6	5.555e-7	2.774e-7	6.129e-8
			S/N 8703		
mean	1.704e-5	-1.10e-6	-6.32e-6	2.817e-8	5.211e-7
maximum	3.739e-3	3.69e-3	2.111e-3	1.645e-3	5.73e-4
minimum	-4.48e-3	-3.57e-3	-1.98e-3	-1.83e-3	-5.73e-4
variance	3.225e-6	1.673e-6	7.707e-7	5.416e-7	6.822e-8

	410Lu	441Lu	488Lu	520Lu	683Lu
			S/N 8702		
mean	-4.23e-8	-4.79e-7	1.690e-7	7.042e-8	-2.82e-8
maximum	4.86e-4	3.5e-4	5.46e-4	9.5e-5	3.3e-5
minimum	-1.24e-4	-1.98e-4	-3.73e-4	-2.7e-5	-3.9e-5
variance	1.188e-8	1.523e-8	2.306e-8	4.76e-10	1.68e-10
			S/N 8703		
mean	8.451e-8	-1.27e-7	7.042e-8	2.817e-8	2.817e-8
maximum	8.3e-5	7.7e-5	4e-5	5.6e-5	2.6e-5
minimum	-5.5e-5	-9e-5	-2.8e-5	-5.1e-5	-3.2e-5
variance	1.079e-9	1.358e-9	1.91e-10	4.36e-10	1.17e-10

The Biowatt deployment coincided with a test deployment at the Scripps Canyon site of an MER-2020 being used by Biospherical Instruments to test new sensors for the measurement of "Natural Fluorescence". Figure 12 shows plots of downwelling irradiance from these three instruments on April 18, 1987. It is interesting to note that this plot shows simultaneous data taken at three locations on that day. Two of the locations were in the mid north Atlantic while one was in the Pacific coastal region. We also can look back on that Pacific site (Scripps Canyon) and find data for the same period in 1984 and 1986. If we had satellite data for these periods, then these data could be useful in calibration and degradation studies.

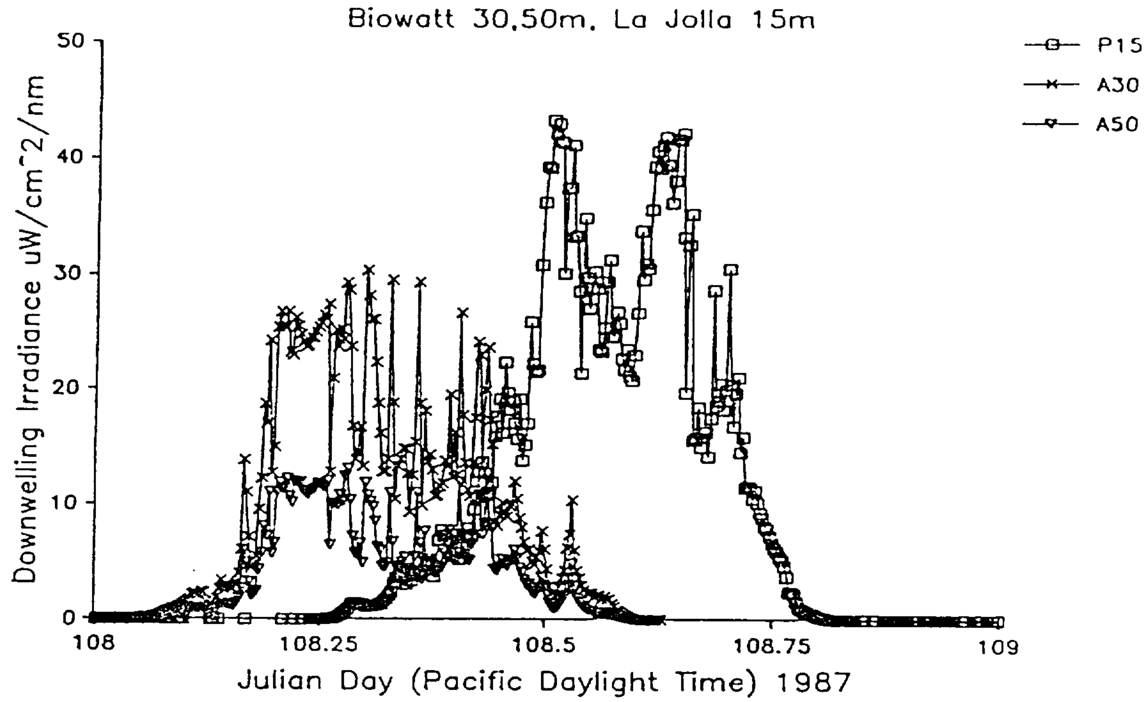

Figure 21a: MER-2020 Mooring on April 18, 1987. Simultaneous data are from two MER-2020s deployed in the Alantic and one deployed in the Pacific at the Scripps Canyon site. $E_d(488)$ shown.

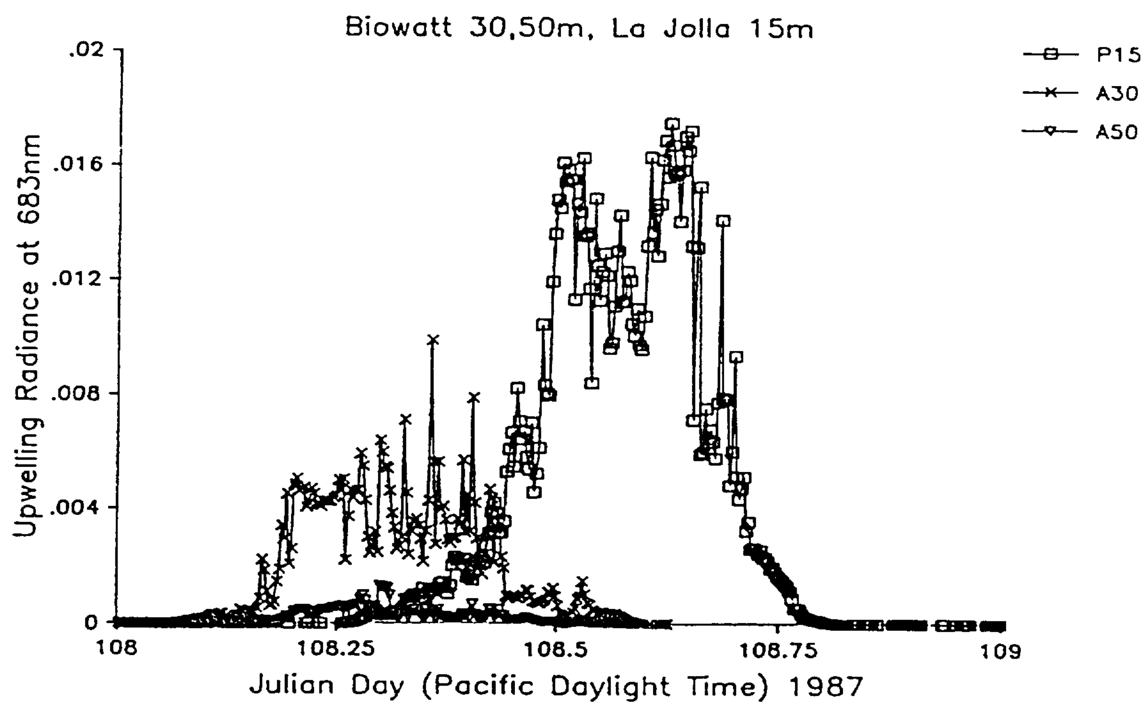

Figure 21b: Same sensors as above, but plotting L_u683, also believed to be gross primary production.

VI. Summary

The project to develop moored spectroradiometers was a success on several different levels. We have succeeded in conducting two long term moorings of an optical testbed. From this experience we have designed and built a moorable spectroradiometer called the MER-2020. We have also sold and delivered the first production run of this instrument and seen it successfully used in a long term deep water mooring; it is still deployed in the Summer of 1987.

The data sets obtained during the two moorings are being analyzed by investigators at different institutions and we are involved in a data analysis project funded by NASA through Scripps. These sets are unique in several ways. Specifically, at a minimum of three wavelengths we acquired data on up and downwelling irradiance, up and downwelling scalar irradiance, and upwelling radiance, and to a more limited extent, the diffuse attenuation coefficient of downwelling irradiance, all on a continuous (daytime) basis. This will enable testing certain properties of radiative transfer such as the distribution functions for usefulness in remote sensing.

Many other problems in ocean optics can be addressed with data collected during these moorings. We can now test how inherent the "apparent" optical properties are. We can look at the remote sensing algorithms developed over the past fifteen years of investigations and apply them as a function of depth, cloud cover, and sun angle, in addition to biological components of the water.

This project has had "spin-offs" in addition to the those described above. The internal electronics of the MER-2020 as been adapted for a bioluminescence detector funded by ONR. The initial moorings let to our realization that $L_u(683)$ or "Natural Fluorescence" might be a powerful predictor of primary production.

The simultaneous data presented in figure 21 shows how powerful multiple moored spectroradiometers can be. It is possible for a single researcher to deploy moored spectroradiometers configured for bio-optical measurements in vertical or horizontal arrays, or even in different oceans. Now it is up to Congress to enable NASA and NOAA to launch the new ocean color satellites to put this new technology to work.

VII. Acknowledgments

This project was made possible by contracts sponsored by NASA under the Small Business Innovational Research Program; contract numbers NAS7-923 and NAS 7-934. We would like to thank Don Collins (JPL), Ray Smith (UCSB) and Dick Eppley (SIO), for their useful discussions and encouragement. We particularly thank Dick Eppley and Ed Renger for their support in the field sampling during the first mooring. The Food Chain Research Group at Scripps also supported this project with the loan of equipment, as did Ray Smith. The Scripps moorings would not have been possible without the efforts of Ron McConnaughey and Charlie Arneson (both of SIO).

Photosynthetic pigments were measured by Maria Vernet at Scripps although this was not funded under the contract. The addition of these measurements significantly increases the value of the data set.

At Biospherical Instruments the microprocessor based design was done by Marv Elston and mechanical design by Mehdi Attaran. Basil D'Sousa was in charge of the collectin data and inventorying. Various other personnel both at Scripps and Biospherical were also crucial.

The BIOWATT program, organized by Eric Hartwig of ONR with John Marra (Lamont) as chief scientist, provided a proving ground for Ray Smith (UCSB) to deploy the MER-2020s.

Finally, we (CRB) owe a big debt to Rudy Preisendorfer at PMEL who provided many extensive written discussions about our observations of the underwater light field. Many fields of science feel a great loss at his passing.

Appendix I: References

Abbott, M.R., P.J.Richerson, and T.M.Powell (1982):"In situ response of phytoplankton fluorescence to rapid variations in light", Limnol. Oceanogr. 27(2), 218-225.

Baker, K.S, and R.C.Smith (1979): Quasi-inherent characteristics of the diffuse attenuation coefficient for irradiance. Proc. Soc. Photo-Optical Instrumentation Engineers, 208, pp.60-63.

Booth, C. R. and P. Dustan (1979): "Diver-Operable Multiwavelength Radiometer", Proc. Society of Photo-Optical Instrumentation Engineers, SPIE V. 196.

Booth, C.R. (1976):"The design and evaluation of a measurement system for photosynthetically active quantum scalar irradiance", Limnol. Oceanogr. 21(2), 326-336.

Bukata, R.P., J.H. Jerome, J.E. Bruton, S.C. Jain and H.H. Zwick (1981): "Optical water quality model of lake Ontario...", Applied Optics, 20(9), 1689-1714.

Gordon, H.R., R.C.Smith, J.R.V.Zaneveld (1984): "Introduction to Ocean Optics", in Ocean Optics VII, M. A. Blizard, ed., Proc SPIE 489, 2-41.

Gordon, H.R., and W.R.McCluney (1975):"Estimation of the depth of sunlight penetration in the sea for remote sensing", Applied Optics, 14(2), 413-416.

Holm-Hansen, O.,C.J.Lorenzen, R.W.Holmes, and J.D.H. Strickland (1965): "Fluorometric determination of chlorophyll",J.Cons.Perm. Int.Explor. Mer 30, 3-15.

Kirk, J.T.O. (1984):"Dependence of relationship between inherent and apparent optical properties of water on solar altitude", Limnol. Oceanogr. 29(2), 350-356.

Kishino, M., C.R.Booth, and N. Okami (1984): "Underwater radiant energy absorbed by phytoplankton, detritus, dissolved organic matter and pure water", Limnol. Oceanogr. 29(2), 340-349.

MAREX (1982): "The marine resources experiment program (MAREX): Report of the Ocean Color Science Working Group";NASA publication, J.J.Walsh, Chairman.

Marra, J. and K. Heinemann (1982):"Photosynthesis response by phytoplankton to sunlight variability";Limnol.Oceanogr.,27(6),1141-1153.

Mitchell, B.G. and D.A.Kiefer (1984): "Determination of the Absorption and Fluorescence Execitation Spectra for Phytoplankton", Marine Phytoplankton and Productivity. O. Holm-Hansen, L. Bolis and R.Gilles, ed. Springer, 157-169.

Nealson,K.H., A.C.Arneson, and A.Bratkovich (1984):"Preliminary results from studies of nocturnal bioluminescence with subsurface moored photometers", Marine Biology 83,185-191.
Plant Physiology.
Smith, R.C. et. al.(1980): "Ultraviolet submersible spectroradiometer" SPIE vol. 208, OceanOptics vol. 1.

Smith, R.C., C.R.Booth and J.L.Star (1984): "Oceanographic Bio-Optical Profiling System", Applied Optics (23), pp. 2791-2797.

Smith, R.C., R.W. Eppley and K.S.Baker (1982a):"Correlation of primary production as measured aboard ship in southern California coastal waters and as estimated from satellite chlorophyll images", Marine Biology, 66, 281-288.

Smith, R.C., (1969):"An underwater spectral irradiance collector"; J. Marine Res. 27:341-350.

Steward, D.E. and F.H.Farmer, 1984. "Extraction, identification, and quantitation of phycobiliproteins pigments from phototrophic plankton", Limnol. and Oceanogr. 29(2) pp 392-397.

Tyler, J.E. and R.C. Smith (1966): "Submersible Spectroradiometer": Opt. Soc. Am. J. 56(10):1390-1396.

Vernet, M. and C.J.Lorenzen, (1987). "The presence of chlorophyll *b* and the estimetino of phaeopigments in marine phytoplankton." J. Planktion Res. 92, pp 255-265.

Vernet. M., B.G.Mitchell, O. Holm-Hansen, and C.R.Booth (1986), "Phycoerithern in planktoin off Scripps Pier": EOS 67(44), p 979.

Warner, J.A., R.W.Austin, D.Bailey, G.Huszar, R.R.McConnaughey, K.Nealson, E.A.Stephan (1983):"Scripps canyon sea structure: a design and deployment for the study of oceanic bioluminescence", Marine Tech. Soc.J., 17(4), 40-47.

APPENDIX II: November 85-June 86 Mooring Data Catalog

DATE MM/DD/YY	MOORING FILENAME	START TIME	STOP TIME	TOTAL SCANS	PLATFORM ANGLE	SAMPLE DELAY
11/ 2/85	M110285B	10:38:0.0	14:55:38.0	886	4.4	60.0
11/ 4/85	M110485H	20:03:17.6	08:03:17.6	25	.7	1800.0
11/13/85	M111385A	15:09:52.6	15:12:12.6	137	3.7	1.0
	M111385B	15:14:31.0	17:24:41.0	772	3.2	10.0
	M111385C	15:40:16.8	17:45:16.8	31	2.7	10.0
	M111385D	NO CASTCARD			.0	.0
	M111385E	NO CASTCARD			.0	.0
	M111385F	17:50:54.3	17:55:21.5	264	3.9	1.0
	M111385G	17:58:35.0	18:01:25.0	18	3.0	10.0
11/14/85	M111485A	23:07:44.5	23:09:04.5	4	3.3	20.0
	M111485B	23:17:24.9	23:26:24.9	8	4.2	60.0
	M111485C	23:30:58.4	17:29:58.4	1078	5.2	60.0
11/15/85	M111585A	19:49:27.9	10:56:27.9	908	4.9	60.0
11/16/85	M111685A	10:58:53.0	11:06:22.7	1106	4.9	.4
	M111685B	16:06:03.5	16:09:29.5	409	4.1	.5
	M111685C	16:21:15.0	18:00:15.0	1540	4.8	60.0
11/17/85	M111785A	18:24:22.5	18:25:44.9	205	4.8	.4
	M111785B	----	----	0	.0	150.0
	M111785C	18:36:48.1	17:34:18.1	1102	6.0	75.0
11/18/85	M111885A	----	----	0	.0	150.0
	M111885B	----	----	0	.0	150.0
	M111885C	19:51:53.6	19:59:23.6	3	5.6	150.0
	M111885D	----	----	0	.0	150.0
	M111885E	----	----	0	.0	150.0
	M111885F	20:25:31.5	20:25:31.5	0	.0	150.0
	M111885G	----	----	0	.0	150.0
	M111885H	----	----	0	.0	150.0
	M111885I	20:44:48.3	17:42:18.3	1080	7.8	150.0
11/20/85	M112085A	18:02:55.9	18:02:55.9	0	.0	150.0
	M112085B	----	----	0	.0	150.0
	M112085C	18:40:39.1	18:40:39.1	1	.0	150.0
	M112085D	18:53:28.7	19:25:58.7	590	14.0	150.0
11/21/85	M112185A	19:34:28.2	19:34:28.2	1	.0	150.0
	M112185B	19:46:44.9	18:19:14.9	1694	15.6	150.0
11/24/85	M112485A	18:38:25.6	TERMINATED	876	19.9	150.0
11/26/85	M112685A	12:10:47.1	12:17:51.5	1029	15.2	.4
	M112685B	12:23:32.5	12:40:21.5	6	3.6	150.0
	M112685C	12:56:38.2	16:49:08.2	94	4.5	150.0
	M112685D	17:17:22.9	17:17:22.9	0	.0	150.0
	M112685E	17:28:30.4	17:03:30.4	567	4.8	150.0
11/27/85	M112785A	17:33:24.4	17:13:24.4	1721	5.7	150.0
11/30/85	M113085A	17:34:04.6	13:31:34.6	1056	4.9	150.0
12/ 2/85	M120285A	13:35:24.7	13:49:38.6	2051	6.6	.4
	M120285B	13:51:55.3	14:16:15.3	147	6.3	10.0
	M120285C	14:18:01.2	14:32:18.4	2053	3.8	.4
	M120285D	14:38:15.9	17:58:15.9	657	6.1	150.0
12/ 3/85	M120385A	18:53:17.8	14:03:17.8	461	7.1	150.0

APPENDIX II: November 85-June 86 Mooring Data Catalog (continued)

DATE MM/DD/YY	MOORING FILENAME	START TIME	STOP TIME	TOTAL SCANS	PLATFORM ANGLE	SAMPLE DELAY
12/ 4/85	M120485A	14:05:57.2	14:19:55.7	2051	19.0	.4
	M120485B	14:21:48.8	14:43:18.8	130	8.5	10.0
	M120485C	14:45:09.1	14:59:14.3	2061	7.8	.4
	M120485D	15:06:45.0	17:09:15.0	1778	10.5	150.0
12/ 7/85	M120785A	17:13:14.8	17:15:06.4	270	17.7	.4
	M120785B	11:38:03.1	07:26:40.0	305	16.9	150.0
12/10/85	M121085A	08:25:49.3	-----	1	.0	150.0
	M121085B	09:21:33.7	09:21:33.7	1	50.3	1.0
	M121085C	09:27:03.1	-----	1	.0	150.0
	M121085D	09:40:39.0	09:40:39.0	1	.0	80.0
	M121085E	-----	-----	0	.0	150.0
	M121085F	14:06:47.2	14:20:49.2	2051	56.6	.4
	M121085G	-----	-----	0	.0	10.0
	M121085H	14:32:58.2	14:38:43.8	13	49.6	10.0
	M121085I	14:41:18.4	14:55:24.8	2051	53.9	.4
	M121085J	15:01:12.5	-----	1	.0	150.0
	M121085K	-----	-----	117	53.9	150.0
12/11/85	M121185A	10:16:34.7	16:11:34.7	142	6.3	150.0
	M121185B	16:15:29.3	16:22:36.3	1035	3.8	.4
	M121185C	16:24:26.1	17:03:56.5	238	2.0	10.0
	M121185D	17:06:27.4	17:17:15.1	1563	3.4	.4
	M121185E	17:23:09.2	17:45:39.2	1162	1.4	150.0
12/13/85	M121385A	18:00:25.2	11:42:55.2	1577	3.0	150.0
12/16/85	M121685A	11:47:47.4	12:02:19.5	2058	5.9	.4
	M121685B	12:08:28.7	19:43:28.7	183	4.2	150.0
	M121685C	19:48:24.6	19:50:21.1	278	3.2	.4
12/19/85	M121985A	12:02:06.8	12:16:30.1	2055	2.7	.4
	M121985B	12:22:32.1	13:30:02.1	27	3.0	150.0
	M121985C	13:32:05.0	13:46:38.6	2053	2.3	.4
	M121985D	13:52:33.1	14:27:33.1	15	3.2	150.0
	M121985E	14:31:50.6	14:46:11.4	2054	4.4	.4
	M121985F	14:51:43.3	15:01:43.4	5	2.5	150.0
	M121985G	15:05:24.3	15:19:51.9	2051	4.0	.4
	M121985H	15:25:35.3	15:45:35.3	9	2.5	150.0
	M121985I	15:48:12.4	16:02:49.6	2054	2.8	.4
	M121985J	16:09:00.6	16:34:00.6	11	3.0	150.0
	M121985K	16:38:20.3	16:56:20.3	2573	3.3	.4
	M121985L	18:11:56.4	16:46:56.4	1119	3.5	150.0
12/21/85	M122185A	16:48:39.8	16:53:23.6	645	3.2	.4
	M122185B	16:59:41.1	18:52:11.1	1198	3.9	150.0
12/23/85	M122385A	18:56:40.7	18:58:28.9	262	2.8	.4
	M122385B	19:04:19.1	16:49:19.1	1675	5.0	150.0
12/26/85	M122685A	18:30:29.0	16:20:29.0	2253	5.3	150.0
12/30/85	M123085A	16:23:03.3	16:25:50.5	504	6.1	.4
	M123085B	18:10:38.1	16:33:08.1	1690	6.7	150.0
1/ 2/86	M010286A	16:36:53.3	16:39:37.5	404	10.3	.4
	M010286B	17:14:24.7	16:36:54.7	1714	8.4	150.0

APPENDIX II: November 85-June 86 Mooring Data Catalog (continued)

DATE MM/DD/YY	MOORING FILENAME	START TIME	STOP TIME	TOTAL SCANS	PLATFORM ANGLE	SAMPLE DELAY
1/ 5/86	M010586A	16:53:11.6	16:54:54.7	253	13.0	.4
	M010586B	17:02:40.1	09:40:10.1	1552	13.8	150.0
1/ 8/86	M010886A	09:42:14.3	09:56:16.3	2052	2.6	.4
	M010886B	10:23:41.1	20:06:11.1	1962	12.1	150.0
1/11/86	M011186A	20:17:27.0	17:54:57.0	1672	18.0	150.0
1/14/86	M011486A	17:57:24.6	17:59:14.5	268	24.3	.4
	M011486B	18:45:33.0	11:23:03.0	976	16.8	150.0
1/16/86	M011686A	11:26:03.1	11:40:16.7	2087	23.4	.4
	M011686B	11:47:29.7	16:47:29.7	1273	23.7	150.0
1/18/86	M011886A	16:51:05.9	16:53:07.3	297	11.5	.4
	M011886B	17:39:31.3	16:27:01.3	1699	27.5	150.0
1/21/86	M012186A	16:30:36.5	16:32:20.5	257	42.5	.4
	M012186B	17:20:10.1	12:35:10.1	361	34.5	150.0
1/22/86	M012286A	12:38:37.9	12:58:38.2	2931	38.5	.4
	M012286B	13:04:11.1	13:29:11.1	11	32.0	150.0
	M012286C	13:31:48.8	13:35:03.3	473	43.0	.4
	M012286D	13:40:03.7	17:43:03.7	661	35.2	150.0
1/23/86	M012386A	17:50:31.3	17:38:01.3	558	40.5	150.0
1/24/86	M012486A	17:41:13.5	17:45:36.7	640	29.3	.4
	M012486B	17:51:03.1	10:11:03.1	1545	41.4	150.0
1/27/86	M012786A	10:18:32.8	17:51:02.8	182	13.4	150.0
	M012786B	17:54:02.3	17:56:02.3	292	2.4	.4
	M012786C	18:37:58.5	17:47:58.5	957	2.6	150.0
1/29/86	M012986A	17:56:01.3	17:06:01.3	1709	2.3	150.0
2/ 1/86	M020186A	17:10:13.0	17:11:54.6	250	9.9	.4
	M020186B	18:31:48.2	12:49:18.2	970	2.8	150.0
2/ 3/86	M020386A	18:19:47.1	18:29:50.5	1466	3.5	.4
	M020386B	18:35:40.1	18:40:56.3	769	22.4	.4
	M020386C	18:47:14.0	10:47:14.0	384	6.0	150.0
2/ 4/86	M020486A	10:51:22.6	10:58:26.5	1029	15.4	.4
	M020486B	11:04:23.5	13:54:23.5	68	2.3	150.0
	M020486C	13:58:34.3	14:05:40.4	1034	6.5	.4
	M020486D	14:11:14.4	16:33:44.4	55	3.0	150.0
	M020486E	16:36:02.2	16:44:23.7	1211	19.2	.4
	M020486F	16:52:12.5	09:32:12.5	344	5.1	150.0
2/ 5/86	M020586A	10:29:53.8	10:37:45.9	1138	13.4	.4
	M020586B	10:43:33.7	10:51:03.7	4	6.3	150.0
	M020586C	11:03:07.6	15:05:37.6	2402	6.1	150.0
2/ 9/86	M020986A	15:09:17.6	15:16:32.9	1048	42.8	.4
	M020986B	15:22:40.4	17:10:10.4	620	41.5	150.0
2/10/86	M021086A	17:25:09.2	17:26:54.9	254	37.7	.4
	M021086B	18:38:25.2	17:05:55.2	540	40.4	150.0
2/11/86	M021186A	17:10:16.9	17:12:04.0	265	2.0	.4
	M021186B	18:21:10.8	13:43:40.8	1042	1.8	150.0
2/13/86	M021386A	13:47:06.5	14:01:39.7	2129	8.8	.4
	M021386B	14:07:08.5	12:47:08.5	854	4.4	150.0

APPENDIX II: November 85-June 86 Mooring Data Catalog (continued)

DATE MM/DD/YY	MOORING FILENAME	START TIME	STOP TIME	TOTAL SCANS	PLATFORM ANGLE	SAMPLE DELAY
2/15/86	M021586A	12:54:12.3	12:55:02.3	6	2.6	10.0
	M021586B	12:56:55.3	13:04:39.6	1116	5.0	.4
	M021586C	13:06:16.4	13:14:21.1	938	5.6	.4
	M021586D	13:19:53.9	11:49:53.9	541	3.6	150.0
2/16/86	M021686A	11:52:35.7	12:04:13.5	1663	3.6	.4
	M021686B	12:09:58.3	17:47:28.3	1288	4.6	150.0
2/18/86	M021886A	17:51:27.8	17:53:14.8	255	4.9	.4
	M021886B	18:51:02.7	17:18:32.7	3420	3.7	150.0
2/24/86	M022486A	17:22:11.3	17:23:56.7	257	8.2	.4
	M022486B	18:52:18.8	11:59:48.8	3868	5.7	150.0
3/ 3/86	M030386A	12:17:34.2	12:24:37.1	1026	3.0	.4
	M030386B	13:59:27.7	17:36:57.7	88	2.4	150.0
	M030386C	19:01:54.4	17:11:54.4	2261	2.3	150.0
3/ 7/86	M030786A	17:19:09.7	16:59:09.7	2297	5.1	150.0
3/11/86	M031186A	17:02:51.3	17:04:35.1	253	15.2	.4
	M031186B	19:09:20.3	17:49:20.3	4001	45.2	150.0
3/18/86	M031886A	18:52:26.8	11:27:26.8	975	45.2	150.0
3/20/86	M032086A	11:30:12.9	11:37:14.3	1026	3.1	.4
	M032086B	11:39:15.7	12:23:15.7	133	4.2	20.0
	M032086C	12:24:52.6	12:31:54.7	1026	7.5	.4
	M032086D	12:34:09.4	12:47:49.4	42	4.2	20.0
	M032086E	12:49:31.8	12:56:34.6	1026	3.7	.4
	M032086F	12:58:31.4	13:23:51.4	77	4.1	20.0
	M032086G	13:25:46.5	13:32:50.0	1026	6.6	.4
	M032086H	13:34:49.3	14:22:09.3	143	3.2	20.0
	M032086I	14:25:54.5	14:32:58.5	1026	4.8	.4
	M032086J	14:35:20.6	15:28:40.6	161	2.2	20.0
	M032086K	15:33:59.8	15:41:04.3	1026	4.4	.4
	M032086L	15:45:22.8	16:21:42.8	110	2.2	20.0
	M032086M	16:23:51.1	16:30:55.9	1026	3.0	.4
	M032086N	----------	----------	0	.0	150.0
	M032086O	16:36:45.7	16:51:45.7	46	1.5	20.0
	M032086P	16:54:21.3	17:01:26.9	1026	4.2	.4
	M032086Q	17:03:52.0	17:20:32.0	51	.9	20.0
	M032086R	17:23:07.2	17:30:13.9	1026	5.6	.4
	M032086S	17:32:39.8	17:50:39.8	55	1.7	20.0
	M032086T	17:53:08.8	18:00:15.8	1026	2.5	.4
	M032086U	18:02:45.6	18:18:25.6	48	2.1	20.0
	M032086V	18:29:19.7	12:57:44.3	5708	3.5	150.0
4/ 1/86	M040186A	18:06:08.9	09:18:38.9	366	10.1	150.0
4/ 2/86	M040286A	09:25:42.9	10:45:42.9	2337	10.7	150.0
4/ 6/86	M040686A	10:58:10.9	13:28:10.9	1213	11.9	150.0
4/ 8/86	M040886A	16:20:58.4	13:30:58.4	2813	15.2	150.0
4/13/86	M041386A	13:38:21.0	19:23:21.0	4171	14.6	150.0
4/20/86	M042086A	19:31:40.9	19:41:40.9	1157	19.4	150.0
4/22/86	M042286A	20:36:38.3	15:54:08.3	464	5.3	150.0
4/23/86	M042386A	16:26:18.1	15:48:48.1	3442	4.4	150.0
4/29/86	M042986A	15:56:38.7	09:56:38.7	1009	45.6	150.0

APPENDIX II: November 85-June 86 Mooring Data Catalog (continued)

DATE MM/DD/YY	MOORING FILENAME	START TIME	STOP TIME	TOTAL SCANS	PLATFORM ANGLE	SAMPLE DELAY
5/ 1/86	M050186A	11:28:29.1	21:28:29.1	3121	4.0	150.0
5/13/86	M051386A	18:43:48.5	14:08:06.4	4496	8.4	150.0
5/21/86	M052186A	15:44:16.4	10:14:16.4	445	14.0	150.0
5/22/86	M052286A	10:19:29.0	16:16:59.0	3600	15.6	150.0
5/28/86	M052886A	17:47:24.9	12:54:54.9	1036	16.6	150.0
5/30/86	M053086A	13:19:36.6	08:59:36.6	3929	17.2	150.0
6/ 6/86	M060686A	09:06:58.7	17:41:58.7	3663	16.8	150.0
6/12/86	M061286A	17:51:16.4	15:11:16.4	2816	15.1	150.0
6/17/86	M061786A	18:58:29.9	18:58:29.9	1	.0	150.0
	M061786B	19:07:32.0	17:07:32.0	529	15.8	150.0
6/18/86	M061886A	19:54:45.3	08:47:15.3	2614	15.5	150.0

APPENDIX III: November 85-May 86 Vertical Profiles

DATE MM/DD/YY	VERTICAL FILENAME	MOORING FILENAME	MREC #	START TIME	TOTAL SCANS	CLOUD CONDITION
10/15/85	V101585A		---	11:32:11	436	100% CLEAR
10/29/85	V102985A		---	9:06:54	399	OVERCAST
	V102985B		---	9:18:27	1316	OVERCAST
	V102985C		---	9:42:47	1171	OVERCAST
	V102985D		---	10:01:05	493	OVERCAST
11/ 5/85	V110585A	M110485H	---	9:21:01	27	90% CLEAR
	V110585B	M110485H	---	9:23:25	2622	90% CLOUDS
	V110585C	M110485H	---	10:02:24	639	90% CLOUDS
	V110585D	M110485H	---	10:14:45	480	90% CLOUDS
11/13/85	V111385A	M111385A	22	15:52:23	1195	CLEAR
11/19/85	V111985A	M111885I	312	9:47:14	195	99% CLEAR
11/26/85	V112685A	M112485A	---	09:04:43	210	50% THIN CLOUDS
	V112685B	M112485A	---	10:13:54	131	100% CLEAR.CALM
12/10/86	V121085A	M121085F	1	14:06:55	203	85% CLEAR,15% NIMBUS
	V121085B	M121085F	512	14:10:46	174	CLEAR
12/11/85	V121185A	M121185A	92	14:07:07	161	95% CLEAR+THIN CIRRUS
	V121185B	M121185B	96	14:11:16	135	95% CLEAR+CIRRUS
12/12/85	V121285A	M121185E	381	9:14:56	158	100% CLEAR,2' SWELL
	V121285B	M121185E	382	9:19:20	158	100% CLEAR,2'SWELL
12/18/85	V121885A	M121685C	---	11:01:34	121	CLEAR
	V121885C	M121685C	---	11:57:02	89	CLEAR
12/19/86	V121985A	M121685C	---	09:42:40	125	100% CLEAR,NO SWELL
	V121985B	M121685C	---	09:45:48	240	100% CLEAR,NO SWELL
12/20/85	V122085A	M121985L	371	9:38:40	197	CLEAR
	V122085B	M121985L	372	9:43:46	176	CLEAR
1/ 7/86	V010786A	M010586B	971	09:26:05	254	100% CLEAR
1/ 8/86	V010886A	M010586B	154	09:18:45	98	CLEAR
	V010886C	M010586B	154	09:24:02	149	CLEAR
1/13/86	V011386A	M011186A	882	09:06:14	149	80% THIN CIRRUS
1/22/86	V012286B	M012186B	290	09:37:32	202	95% mostly CLOUDS
1/29/86	V012986B	M012786C	773	10:06:48	209	80% THIN CIRRUS
1/31/86	V013186A	M012986A	965	10:06:25	114	90% THICK CLOUDS
2/10/86	V021086A	M020986B	531	13:32:33	83	CLEAR
	V021086B	M020986B	534	13:35:25	160	CLEAR
2/12/86	V021286A	M021186B	352	09:03:54	94	HIGH CLOUDS
	V021286B	M021186B	---	--------		
2/13/86	V021386A	M021186B	977	11:00:41	124	100% OVERCAST
	V021386B	M021186B	978	11:05:18	212	100% OVERCAST
	V021386C	M021386A	995	11:50:44	290	
2/19/86	V021986A	M021886B	374	10:25:19	239	100% OVERCAST
	V021986B	M021886B	367	10:06:06	291	100% OVERCAST
2/20/86	V022086A	M021886B	968	11:08:08	117	95% CLEAR
	V022086B	M021186B	970	11:15:47	331	95% CLEAR
2/27/86	V022786A	M022486B	151	09:55:39	112	100% OVERCAST/FOG
	V022786B	M022486B	151	09:59:49	222	100% CLOUDY/FOG
2/28/86	V022886A	M022486B	208	09:34:32	128	100% OVERCAST/FOG
	V022886B	M022486B	208	09:37:57	251	100% OVERCAST/FOG

nstruments Inc.
n Moored Spectroradiometers

	ICAL FILENAME	MOORING FILENAME	MREC #	START TIME	TOTAL SCANS	CLOUD CONDITION
	30486A	M030386C	339	09:06:19	151	100% CLOUDY
	030486B	M030386C	345	09:22:00	214	100% CLOUDY
	030686A	M030386C	149	09:09:44	120	100% CLOUDY
	V030686B	M030386C	149	09:19:39	229	100% CLOUDY
	V032086A	M031886A	912	08:49:40	144	100% CLEAR
	V032086B	M031886A	914	08:54:29	258	100% CLEAR
	V032086C	M031886A	960	10:51:06	298	100% CLEAR
	V032086D	M032086B	94	12:10:17	285	100% CLEAR
	V032086E	M032086D	27	12:42:47	589	100% CLEAR
	V032086F	M032086H	1	13:34:38	280	100% CLEAR
	V032086G	M032086J	1	14:36:01	269	CLEAR
	V032086H	M032086J	1	15:28:13	275	CLEAR
	V032086I	M032086M	1	16:23:00	337	100% CLEAR
21/86	V032186A	M032086V	450	13:13:23	114	100% CLEAR
	V032186B	M032086V	454	13:21:26	197	100% CLEAR
3/25/86	V032586A	M032086V	270	11:14:48	115	100% CLEAR
	V032586B	M032086V	270	11:19:12	156	100% CLEAR
	V032685A	M032086V	322	08:58:48	100	100% CLEAR
	V032685B	M032086V	322	09:03:02	146	90% CUMULUS CLOUDS
4/ 2/86	V040286A	M040186A	337	08:06:32	101	90% CUMULUS CLOUDS
	V040286B	M040186A	339	08:11:08	134	95% CLEAR
4/16/86	V041686A	M041386A	162	09:23:15	154	95% CLEAR
	V041686B	M041386A	162	09:30:05	232	85% HIGH CIRRUS
5/ 1/86	V050186A	M042986A	987	09:02:26	147	85% HIGH CIRRUS
	V050186B	M042986A	990	09:10:38	183	100% CLEAR
5/ 9/86	V050986A	M050686A	144	09:47:30	138	100% CLEAR
	V050986B	M050686A	144	09:53:43	175	100% CLOUDY
5/15/86	V051586A	M051386A	936	09:42:58	166	100% CLOUDY
	V051586B	M051386A	938	09:47:52	223	95% CLEAR
5/23/86	V052386A	M052286A	570	10:03:49	181	95% CLEAR
	V052386B	M052286A	572	10:08:23	217	